Progress reports of individual researchers

Yasuo ASADA *Energy Technology*
Hydrogen Production by Photosynthetic Microorganisms with the use of Hydrogen-Absorving Metals and Biocatalitic Reduction of Isooxsasoles

Tomohiko ASAI *Nanomaterials and Nanodevices*
Control of Self-Organized Magnetized Plasmoids and Their Applications to Nano-Materials and Medical Technologies

Shigeru CHAEN and Tadashi TOJO *Nanomaterials and Nanodevices*
Imaging of Bio-molecule and Cell

Kyoko FUJIWARA and Masayoshi SOMA *Medical*
Development of an E-box targeting Pyrrole-Imidazole polyamide to inhibit cell growth

Noboru FUKUDA, Kosuke SAITO, Jun IGARASHI and Tomohiko ASAI *Medical*
Drug Discovery of Pyrrole-Imidazole (PI) Polyamide by the Chemical Biology and Development of Plasma Medicine for Skin Malignant Melanoma

Hideomi HASHIBA *Quantum Information; Nanomaterials and Nanodevices*
Single Photon Optoelectronics Devices

Takuya HASHIMOTO *Energy Technology*
Development of Materials for Intermediate-Temperature Solid Oxide Fuel Cells

Hiroki IKAKE *Supramolecules and Self-Assembly*
Development of Poly(lactic acid)s Films as Biopolymer, and Applications to New Material Field

Shuichiro INOUE *Quantum Information*
High Fidelity Entanglement Swapping at Telecommunication Wavelengths

Hiroshi ISHIDA *Quantum Theory and Computation*
Electronic Structure Calculation of Crystal Interfaces, Adsorbed Molecules, and Nanostructures

Akiyoshi ITOH, Arata TSUKAMOTO *Information Storage; Supramolecules and Self-Assembly*
Ultra High Density Information Recording Materials on Self Assembled Nano-structured Substrates

Nobuyuki IWATA *Nanomaterials and Nanodevices*
Pursuing the Limits of Nanomaterial-based Photonic and Quantum Technologies

Ken JUDAI *Nanomaterials and Nanodevices*
Preparation of Metallic Clusters in Solution and Applications to Catalysis

Koichiro KANO *Medical*
Actin Cytoskelton Dynamics Control Adipocyte Differentiation Via Regulation of MKL1

Tsugumichi KOSHINAGA *Medical*
Anti-tumor Effect of Inhibition *LIT1* Gene Transcription by using as New Therapeutic Agent

Takeshi KUWAMOTO *Quantum Information*
Experimental Studies for Quantum Memory Using Neutral Atoms

Yoshikazu MASUHIRO *Medical*
Construction of the Escherichia Coli Expression System of the Cell Membrane Permeable iPSCs Induced Factors That Strengthened Proteolysis Resistance

Yoshiaki MATSUMOTO and Takahiko AOYAMA *Medical*
Pharmacokinetic/Pharmacodynamic Analysis of Tumor-localizing Photosensitizing Compounds

Sachiko MATSUSHITA *Supramolecules and Self-Assembly ; Energy Technology*
Self-assembly and Self-organization from the viewpoint of Device-fabrication Methods

Hiroki NAGASE and Takayoshi WATANABE *Medical*
Applied Chemical Biology: Strategy to Cure Cancer Patients

Katsuji NAKAGAWA *Information Storage*
Research for High Density and High Speed Magnetic Recording- Thermally Assisted Magnetic Recording Applying Near Field Optical Light -

Nobuyuki NISHIMIYA *Energy Technology*
Development of Photonic to Chemical Energies Transformation Systems

Shinichiro OHNUKI *Quantum Theory and Computation*
Nano-Electromagnetic Simulation and Its Applications to Plasmonic Devices

Joe OTSUKI *Supramolecules and Self-Assembly; Energy Technology*
Self-Assembled Supramolecules and Their Applications to Energy, Medical, and Information Technologies

Tokuei SAKO *Quantum Theory and Computation*
Comparison of the Structure of Conjugate Fermi Holes in He-like Systems and Artificial Atoms

Kaoru SUZUKI *Nanomaterials and Nanodevices*
Synthesis of Nano-rod Devices with Wide Band Gap Semiconductor Effect

Satosu TAKAHASHI and Daisuke OBINATA *Medical*
The Development of Newly Molecular Targeting Drug for Prostate Cancer by using PI polyamide

Yoshiki TAKANO *Nanomaterials and Nanodevices*
Mechanism of Superconductivity in Layered Fe-based Superconductors and Search of New Superconducting Compounds

Arata TSUKAMOTO, Akiyoshi ITOH *Information Storage; Supramolecules and Self-Assembly*
Ultra Fast Information Recording and Ultra Fast Photo Magnetic Switching

Tsuneki YAMASAKI *Quantum Theory and Computation*
Distribution of Energy Flow by Dielectric Waveguide withRhombic Dielectric Structures along a Middle Layer –Case of Compared with Deformed Rhombic Dielectric Structure–

Hydrogen Production by Photosynthetic Microorganisms with the use of Hydrogen-Absorving Metals and Biocatalitic Reduction of Isooxsasoles

Yasuo ASADA
Energy Technology Group

Hydrogen production by cyanobacteria combined use of hydrogen-absorbing metals and biocatalitic reduction of isooxasoles and acetophenon using photosynthetic bacteria, are studied.

1. Hydrogen production by photosynthetic microorganisms with the use of hydrogen-absorbing metals (Co-works with Prof.Nishimiya, CST, Nihon-Univ.)

The new methods to collect and stimulate hydrogen produced by cyanobacteria with the use of hydrogen-absorbing metals.

The hydrogen gas produced by cyanobacteria, *Spirulina platensis* and *Anabaena cylindrical* was collected with hydrogen-absorbing metals. By reducing hydrogen partial pressure, the hydrogen production by cyanobacteria, was stimulated. *Spirulina platensis* produces hydrogen gas by anaerobic digestion of intracellular glycogen.

However, the stored hydrogen gas is inhibitory for the hydrogen production. By lowering hydrogen partial pressure with the use of hydrogen-absorbing metals, hydrogen production was stimulated.

In this fiscal year, the positive effect of hydrogen-absorbing metals on production by Enterobacter aerogenes (a kind of facultative anaerobic bacteria) was confirmed.

2. Biocatalitic reduction of isooxasoles and acetophenon by photosynthetic bacteria

Biocatalitic and assymetrical reduction of isooxasoles and acetophenons by photosynthetic bacteria are studied.

Intact cells of some cyanobacteria are known to convert isooxasoles to its alcohol form. The responsible enzyme is assumed to be alcohol dehydrogenase(s), but there has been detailed information. The aim of study is to clarify the responsible enzyme and strengthen the activity by genetic engineering.

We have already acquired transconjugant photosynthetic bacterium, *Rhodobacter sphaeroides* RV with three alcohol dehydrogenase (ADH) enzyme genes from the cyanobacterium, *Synechococcus* PCC7942 and one ADH gene from alcohol-assimilating photosynthetic bacterium,

This fiscal year, we tried to analyze ADH activity by activity staining of native electrophoresis. The cell-free extracts from *Rhodopeudomonas palustris* No.7 in the gels was able to oxidize S-form 1-phenyl alcohol to acetophenon but not R-form.

Control of Self-Organized Magnetized Plasmoids and Their Applications to Nano-Materials and Medical Technologies

Tomohiko Asai
Nanomaterials and Nanodevices Group

Self-organized magnetized plasmoid has attractive advantages for the variety of applications because of its wide range of plasma parameters and its ease of control. In this work, applications of the magnetized plasmoid for a rapid thin-film deposition and EUV light source have been proposed and demonstrated. Also, several innovative applications of the plasma formation technique, e.g. medical treatment and muon catalyzed nuclear fusion have been proposed and initiated in this project.

1. Development of high-speed film deposition technique by magnetized coaxial plasma gun

Magnetized Coaxial Plasma Gun (MCPG) has been applied for new alloy film deposition technique. This method realize the generation of metallic thin film with the materials which have high-melting-point (e.g., Ti, Zr …). Generation methods for these materials had been limited to the ion beam assisted vacuum deposition. The optimization of gun operation and the initial experiment with composite material electrode have been successfully performed. The developed technique had been applied for a patent via NUBIC. （"Fast alloy film deposition method", by Tomohiko Asai, Kaoru Suzuki, Nobuyuki Nishimiya, Mikio Takatsu, 2012.9.6 (JP2012-195690）
(Collaboration with Prof. K. Suzuki and Prof. N. Nishimiya)

2. Application of LF Plasma jet for Medical Treatments

The atmospheric-pressure LF (Low Frequency) plasma jet have been investigated to apply for surface modification technique of e.g. CNT composite materials. The application study of the LF jet for medical treatment has recently been initiated. The high energy electron and ions supplied by the LF jet have a potential to be a tool to control chemical balance of cells in addition to the direct effect of hot particles.

In this project, the study is focusing on the application of LF jet on the cancer treatment. The experimental device has been developed (Figure 1) and the initial experiments will be started within this fiscal year.
(Collaboration with Prof. N. Fukuda, Dr. K. Fujiwara, Dr. H. Koguchi (AIST) et al.)

Figure 1. LF jet for a medical applications.

3. High-efficiency method of muon catalyzed fusion

The muon catalyzed fusion (μCF) is one of the nuclear fusion reaction processes caused in a μ-atom. To improve the efficiency of μCF, innovative concept of fusion reactor design has been proposed and preliminary experiments on a super-Alfvénic translated FRC (Field-Reversed Configuration) plasma (Figure 2) have been initiated. (Collaboration with Dr. E. Nakamura, KEK)

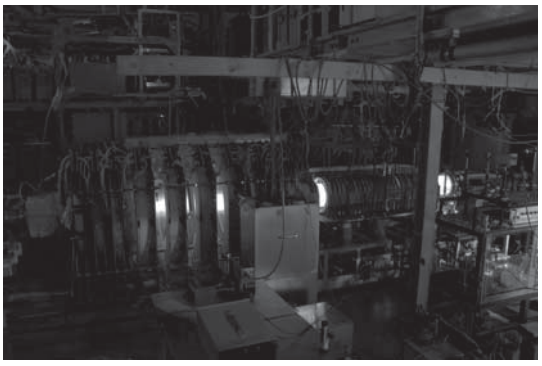

Figure 2. FAT device.

Imaging of Bio-molecule and Cell

Shigeru CHAEN and Tadashi TOJO
Nanomaterials and Nanodevice Group

1. Studies on the biomolecular motor using the ordinary fluorescent imaging technique.

In vitro motility assays using bipolar myosin thick filaments demonstrated that actin filaments slides slower in the direction leading away from the central zone than towards it. Recently, we have suggested that the backward movement causes the myosin heads to be constrained and increase in the energy required for the ADP release step by the findings that the thermal activation energy. In this study, in order to examine whether ADP release rate is slower in the backward than the forward movement, we constructed an assay system to estimate the ADP release rate from the displacement of fluorescent nucleotides bound to myosin heads by flash photolysis of caged ATP. Using the new assay system, we obtained that ADP release rate is slower in the backward than the forward movement. (BIOPHYSICS in press. 2013)

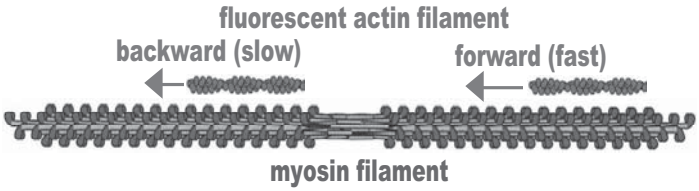

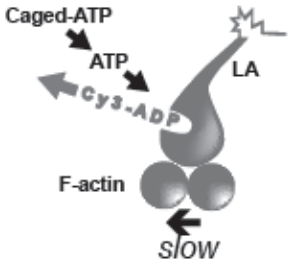

2. Development of a new wet cell using a carbon thin diaphragm to observe a living cell in aqueous solution with Scanning Electron Microscopy at nanometer resolution

In electron microscopy, transparency of specimens against a beam of electrons in TEM or intensity of secondary electrons and so on induced by an incident electron beam in SEM is translated into contrast. Any material surrounding a specimen, which prevents electron beam passing or detection of secondary electrons, obstructs to create an image. Hence, electron microscopy intrinsically requires high voltage electron beam irradiation of specimens and high vacuum under 10-4 Pa in the cell for specimens. Water in samples must be replaced with some resins or completely dried up. These conditions make it difficult to observe wet or living samples like enzymes retaining catalytic activities or living cells in aqueous solution. To image wet and living samples using electron microscopy at nanometer resolution, we are developing a new wet cell for SEM whereby living cells and enzymes can be maintained in aqueous solution. A carbon thin layer with thickness of 20 nm was made by vacuum evaporation. We applied it as a diaphragm withstanding a pressure gap for separating a specimen in solution at atmospheric pressure from high vacuum environment. Cells and enzymes were placed on its surface of the atmospheric side. They were imaged using SEM. The EM photographs show detailed structures of the cell membrane and the enzymes.

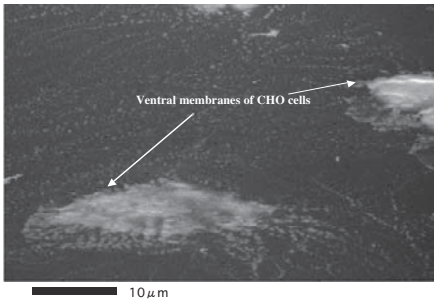

Development of an E-box Targeting Pyrrole-Imidazole Polyamide to Inhibit Cell Growth

Masayoshi SOMA, Kyoko FUJIWARA
Medical Group

The amplification or over expression of c-MYC has been observed in many tumors. c-MYC is a basics-helix-loop-helix leucine zipper transcription factor that binds E-box (5'-CACGTG-3') sequence of DNA with its partner MAX protein. It activates the transcription of more than 4000 genes whose products are involved in crucial aspects of cancer biology such as cell proliferation, cell growth, apoptosis and differentiation. There have been many approaches to down regulate MYC or its downstream genes, however, none of them has been succeeded to be developed as an anti-cancer drugs, because of the lack of drug-delivery system, or too complex treatment procedure.

Pyrrole–imidazole (PI) polyamides can bind to double strand DNA in a sequence specific manner and suppress the expression of target gene by inhibiting DNA binding proteins including transcription factors. PI polyamides are small synthetic molecules composed of the aromatic amino acids N-methylpyrrole (Py) and N-methylimidazole (Im). A pair of PI polyamide recognizes specific DNA base pairs, i.e. Im/Py pair bind to G-C, Py/Im to C-G, and Py/Py to both A-T and T-A. A concatenation of those pairs made it possible to bind to a variety of specific DNA sequences.

We designed several PI polyamides which recognize E-box consensus, and found that one of those PI polyamide Myc-6 inhibits proliferation of the many cells including osteosarcoma cell line MG63. The cells treated with 1mM or higher concentration of Myc-6 showed reduced growth rate when they were examined by WST8 assay and colony formation assay. It was also revealed by wound-healing assay that Myc-6 inhibited cell migration activity dose-dependently. Intravenous injection of Myc-6 at 6 mg/kg body weight once a week for a month caused growth inhibition MG63 xenograft developed in Nude mouse without evidence of toxicity. It was also observed that Myc-6 treatment increased the amount of phosphatidyl serine, which is the marker of early apoptosis, on cell membrane, however, no clear evidence of late apoptosis or necrosis was found.

By global gene expression analysis using Affymetrix GeneChip U133 Plus, 18 genes were found to be significantly down-regulated in MG63 cells treated with 10mM Myc-6. Even though we failed to find the direct target genes of Myc-6 polyamide, we found that extracellular matrix related genes, such as *Collagen 3A1*, *14A1*, *Matrix metalloproteinase 1*, and the genes involved in RNA maturation, such as *MALAT1* and *NEAT1* were down regulated by Myc-6 treatment. Since those genes could be involved in regulating growth and/or migration of tumor cells, and could be a new therapeutic target, we are doing further functional analysis of them.

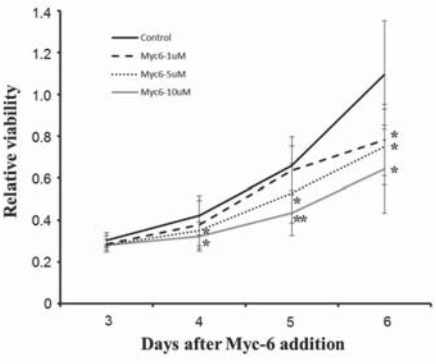

Fig.1 Growth inhibition of MG63 cells by Myc-6 treatment.

Drug Discovery of Pyrrole-Imidazole (PI) Polyamide by the Chemical Biology and Development of Plasma Medicine for Skin Malignant Melanoma

Noboru FUKUDA, Jun IGARASHI, Kousuke SAITO and Tomohiko ASAI
Medical Group

To develop DNA-recognized PI polyamide targeting human TGF-β1 as practical medicines, we tried to determine a lead compound, and provide the preclinical studies using common marmosets. We also develop the Nihon University original methodology to induce iPS cells using the PI polyamide targeting human TGF-β1. Moreover, we started a project of the development of plasma medicine for skin malignant melanoma collaborating with the plasma team in College of Science and Technology.

I. Determination of a lead compound targeting human TGF-β1

Among seven PI polyamides designed to bind on the promoter region of human TGF-β1 gene, we selected GB1101, GB1105, and GB1106, and examined their effects on expression of TGF-β1 mRNA in humen cultured vascular smooth muscles. GB1105 and GB1106 strongly inhibited expression of TGF-β1 mRNA in a dose-dependent manner. We confirmed that GB1101 is strongest to inhibit the expression of TGF-β1 mRNA in human- and marmoset-derived fibroblasts.

II. Establishment of ointment containing PI polyamide targeting human TGF-β1

We start to establish ointment containing PI polyamide targeting human TGF-β1 to develop PI polyamide as a practical medicine for the skin hypertrophic scar collonborating with solution manufacturing room in Nihon University Itabashi Hospital. We checked the combination of components of soluble materials and solutions for PI polyamides and found that Macrogol Ointment was most effective substrate to delivery the PI polyamide into skin.

III. Preclinical study for PI polyamides using common marmosets

The preclical study using the primates is essential to develop PI polyamides. We chose common marmosets that are compact and have a reproductive power for the preclinical study. We examined effects of PI polyamides targeting human TGF-β1 on development of skin finrotic scar created in common marmosets and confirmed acual inhibition of the skin scar.

IV. Development of the Nihon University original methodology to induce iPS cells using the PI polyamide targeting human TGF-β1

1) We evaluated the effect of PI polyamides to induce EMT on human mammary epithelial cell lines by assay for examining cell proliferation and migration activity. As a result, Treated group showed lower expression activity level of TGF-β1 and Snail genes, which are involved in EMT. These results suggest that those PI polyamides may be useful for inhibit EMT in human mammary epithelial cells.
2) Currently, We have tried to induce human iPS to administer to HDF cells proteins, which cell extracts of 293T stable expression cell strains of Flag-Sox2 or Oct4 or Klf4-11R, and Flag-Sox2-Stabilon-11R fusion proteins and 6×His tag conjugated MTM-cMYC fusion protein constructed by *E. coli* expression system, and ①TGF-β1 inhibitors, ②human TGF-β1 specific PI polyamides, ③Apigenin which a flavonoid that increases the expression of E-cadherin, ④TGF-β1 inhibitors and human TGF-β1 specific PI polyamide, ⑤human TGF-β1 specific PI polyamide and Apigenin, when change the human iPS induced medium after reseed the cells on feeder cells.

V. Development of plasma medicine for skin malignant melanoma

We started a project of the development of plasma medicine for skin malignant melanoma collaborating with the plasma team in College of Science and Technology. This plasma medicine targets the cancer stem cell with all trans retinoic acid to reduce the tolelance of radical oxygen species.

Single Photon Optoelectronics Devices

Hideomi HASHIBA
Nanomaterials and Nanodevices Group; Quantum Information Group

Our research aims development of single photon optoelectronic devices. Our research has focused on silicone waveguides for quantum information transport, two dimensional TiO_2 photonic crystals of low refractive index for solar cells, and single photon detectors for THz range this year.

1. Development of fabrication technology of silicone waveguides with ICP etching

Semiconductor wave guides and photonic crystals are increasingly important in optoelectronic devices for quantum information technology. We study silicone wave guide devices with its third-order nonlinearities. Research of silicone wave guide devices of this year has been focused on development of simple fabrication method of the waveguides and we attained to develop concrete fabrication method for a Si waveguide of 320 nm wide and more than 1 mm long. The waveguide has small roughness of side-walls of less than 10 nm and accuracy of shape of the waveguide is restricted by our EBL.

2. Two dimensional TiO_2 photonic crystal as photo sensitized solar cell

Two dimensional phonic crystals (PCs) of titanium oxide (TiO_2) of low refractive index to meet the needs of the advanced solar cells. Our PCs are fabricated with standard electron beam resist mask and deposition techniques of Ag-O_2 mixture gas of 1:1.5 at 1 x 10^{-2} Torr. The patterned TiO_2 film is then baked at 550 degrees and transform amorphous to mixture of rutile and anatase. The observation of the layer under XRD measurement shows that some rutile turns into anatase at that temperature.

3. THz plasma excitations of quantum dots confined with shallow potential barriers

We studied the "Single-electron transistors in THz range". THz range single photon detectors are assembled from a GaAs/AlGaAs quantum dot coupled with a metallic single electron transistor which senses appearance of charge state of the QD. Plasma excitations of the QD arises with a formation of confinement potential barrier from the reservoir having resistances more than resistance quanta, and we revealed that appropriate shape of the barriers lowers dark counts by suppression of flow of hot electrons form the reservoir and reveals higher order excited states. The higher order excited states is expected to have the same plasma frequency of that of the first and shows a heat bath effect of the QD. This will promise high temperature operation of the THz detection.

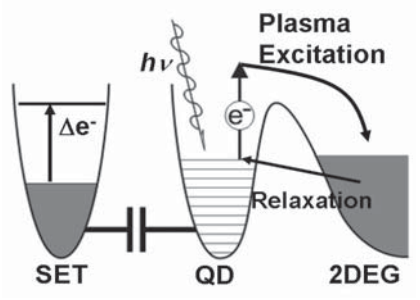

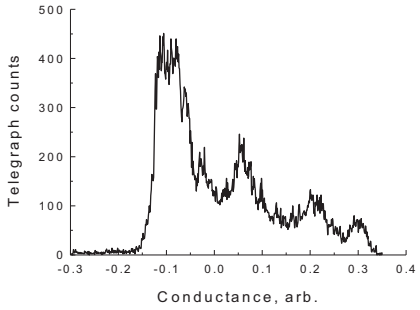

Development of Materials for Intermediate-Temperature Solid Oxide Fuel Cells

Takuya HASHIMOTO
Energy Technology

Solid oxide fuel cells (SOFC) attract much interest due to high efficiency and low emission of pollution gas. At present, operation temperature of SOFC is about 800~1000 °C, which should be reduced to 600~800 °C for practical application. In order to reduce operating temperature, new materials for cathode, electrolyte and anode which work at such a low temperature are necessary. In this year, potential of materials listed below has been examined. Fabrication of SOFC by combination of the examined materials and its evaluation are now in progress.

1. Optimization of preparation method and sintering temperature of $LaNi_{0.6}Fe_{0.4}O_{3-\delta}$ as new cathode material and its stability at low oxygen partial pressures

$LaNi_{0.6}Fe_{0.4}O_{3-\delta}$ attracts interest as new cathode material due to low chemical reactivity with electrolyte material originating from free of Sr. So far, it has been clarified that single phase specimens with high homogeneity and large Ni content can be prepared with one of the solution process, Pechini method instead of frequently employed solid state reaction method. In this year, it has been concluded that sintering of $LaNi_{0.6}Fe_{0.4}O_{3-\delta}$ powder prepared by Pechini method at 1050 °C produces sintering body with sintering density of 70 %, high specific surface area and homogeneous pore size distribution, which are ideal as cathode material. (Mater. Res. Bull. 2013) Comparison of $LaNi_{0.6}Fe_{0.4}O_{3-\delta}$ sintering bodies prepared by other solution processes has been carried out and it has been revealed that Pechini process employed in this study is superior from the viewpoint of controllability of sintering density and homogeneity of pore size distribution. (J. Amer. Ceram. Soc. 2012) For practical application, electrical property under low oxygen partial pressure is also an important factor since cathode is exposed to low oxygen chemical potential under SOFC operation. It has been clarified that $LaNi_{0.6}Fe_{0.4}O_{3-\delta}$ shows electrical conductivity more than 130 $S \cdot cm^{-1}$ below 700 °C despite of oxygen partial pressure as low as 10^{-4} atm

2. Optimization of preparation method and rare earth cation in $BaCe_{1-x}M_xO_{3-\delta}$ (M: rare earth metal)

$BaCe_{1-x}M_xO_{3-\delta}$ (M: rare earth metal) is one of the candidate for alternative electrolyte materials because of high proton conductivity at 400~600 °C. At last year, single phase preparation by Pechini method has been succeeded; however, optimization of rare earth ion has not been performed. In this year, X-ray diffraction measurements at high temperatures under controlled oxygen partial pressures have been performed and rare earth ion in $BaCe_{1-x}M_xO_{3-\delta}$ has been optimized from the viewpoint of structural analysis. For the specimens with M=Y, Sm, Eu, Dy and Yb, only thermal expansion was observed and reduction expansion due to generation of oxide ion vacancy was not detected. For $BaCe_{1-x}Nd_xO_{3-\delta}$, not only thermal expansion but also reduction expansion originating from variation of δ was observed. This indicated that valence of Nd in $BaCe_{1-x}Nd_xO_{3-\delta}$ was tetravalent state at room temperature and varied to trivalent at high temperatures. The valence of Nd thus concluded showed agreement with lower molar volume, δ and proton conductivity than those of other $BaCe_{1-x}M_xO_{3-\delta}$.

3. Preparation of single phase of $Sr_{2-x}La_xFeMO_6$ (M: W, Mo) as new anode materials

For the purpose of preparation of SOFC composed of all perovskite materials, double perovskite oxide which is stable under reductive atmosphere has been examined as anode materials. For the first step, preparation of $Sr_{2-x}La_xFeMO_6$ (M: W, Mo) has been examined and single phase specimens have been prepared. The property as anode materials is now in evaluation.

Development of Poly(lactic acid)s Films as Biopolymer, and Applications to New Material Field

Hiroki IKAKE
Supramolecular and Self-Assembly Group

In our group, the aim of development of poly(lactic acid) (PLA) films as biopolymer with the high thermal- and mechanical- resistance. And then, the improved PLA was submitted to new material field.

1. Development of Poly(*L*-lactic acid) Films with Exhibiting the Piezoelectricity

It is well known that poly(*L*-lactic acid) (PLLA) fibers exhibit the piezoelectricity, in which their piezoelectric constant increases with increasing degree of crystallinity and uniformity of the orientation of the crystallites. Recently, bending motion due to their piezoelectricity has been reported (Fig.1). The *zigzag* motion is closely related to the morphology of PLLA fibers. For this purpose, the irradiated magnetic field, and other process, under the electric field, have produced the high crystalline oriented PLLA films. In the present study, we have successfully synthesized PLLA by using Ring-opening polymerization, and the crystalline of PLLA became the growth by the isothermal crystallization process.

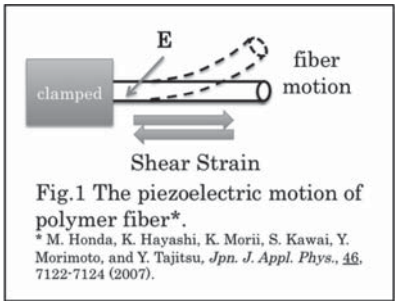

Fig.1 The piezoelectric motion of polymer fiber*.
* M. Honda, K. Hayashi, K. Morii, S. Kawai, Y. Morimoto, and Y. Tajitsu, *Jpn. J. Appl. Phys.*, 46, 7122-7124 (2007).

2. Preparation of High Crystallinity and High Orientation Poly(*L*-lactic acid) Films under Electric Field

Semi-crystallized PLLA has a comparatively low-degree of crystallization (X_c). In order to orient its crystalline domains in a regular way and to raise X_c, electric field was applied to PLLA film while annealing it according to a program. In Fig.2, the dependency of the azimuthal angle for PLLA films at 16.7° caused of the (110)/(200) planes by wide-angle X-ray diffraction. As the results, it was shown that the crystalline domains have oriented in parallel to the direction of the various applied electric field, and the degree of orientation has become increased with increasing applied electric field.

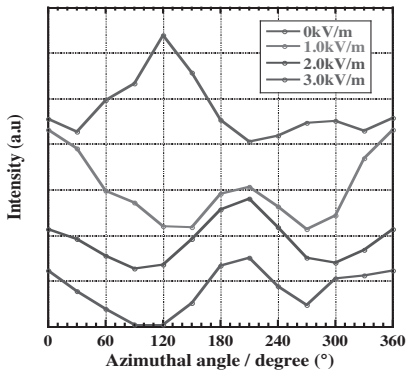

Fig.2 WAXD(110)/(200) intensity along the azimuthal angle for PLLA films.

3. Morphological change of Poly(*L*-lactic acid) Films with Magnetic Irradiation

In this study, we have discussed that the influence of morphological change of PLLA films on magnetic irradiation. The annealing process for PLLA films was the same as in the electric field's program. In the results of small angle X-ray (SAXS) profiles for annealed PLLA films, SAXS peak shifted to lower scattering wave vector: q value with increasing the annealing time at isothermal crystallization process. In Fig.3, the dependency of the annealing temperature for PLLA films at isothermal crystallization process in 0T. As the results, it was shown that the PLLA lamellar thickness have increased with increasing the annealing temperature, but the SAXS peak of annealed PLLA film at 185°C disappeared due to be smaller lamellar thickness with increasing the annealing temperature.

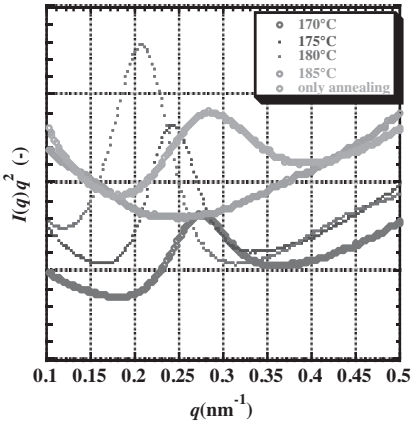

Fig.3 SAXS Lorentz-corrected plots of PLLA films as a function of the annealing temperature at isothermal crystallization.

High Fidelity Entanglement Swapping at Telecommunication Wavelengths

Shuichiro INOUE
Quantum Information Group

Quantum key distribution (QKD) technology has made significant progress in the last decade and the key distribution distance of 200 km has been achieved using a point-to-point QKD system. However, further extension of the key distribution distance using such a system would be difficult, because the error probability scales exponentially with a fiber distance. The promising way to extend the key distribution distance further is to employ quantum repeaters. The preliminary step toward constructing the quantum repeater system is to implement a quantum relay that is a QKD using entanglement distributed via entanglement swapping. In this project, we have demonstrated the high fidelity entanglement swapping at telecommunication wavelengths.

1. Development of polarization entangled photon-pair sources

In the entanglement swapping, it is important to make photons from two independent photon-pair sources indistinguishable. The photons must be identical in their spectral, spatial, polarization, and temporal modes in a Bell-state measurement. The temporal overlap was achieved by the use of synchronized femtosecond pump pulses (approximately 100 fs duration at 79.6 MHz repetition rate) and narrow bandpass filters (FWHM: 4 nm). The pulses have a center wavelength of 775 nm. Two spatially separated 6-mm long type-II periodically poled lithium niobate (PPLN) bulk crystals were pumped by the synchronized pulses and generated cross-polarized photon pairs at 1550 nm via a spontaneous parametric down conversion process. The generated photon pairs were detected by 1.28-GHz sinusoidally gated InGaAs/InP avalanche photodiodes. The visibility of the two-photon interference using each photon-pair source was 87 %. The imperfect visibility was due to the multi photon-pair generation caused by the high pumping.

2. Polarization entanglement swapping

We performed fourfold coincidence measurements to investigate the indistinguishability between photons from the two independent photon-pair sources. The indistinguishability was measured to be 82 % by Hong-Ou-Mandel two-photon interference experiments (Fig.1) Then a partial Bell-state measurement was performed with one photon from each pair, which projected the two remaining photons, formerly independent onto an entangled state. The obtained fidelity of the swapped entangled state was 86 % (Fig. 2), high enough to infer a violation of a Bell-type inequality. Our configuration would be a prototype solution for use in future quantum relay and quantum repeaters over long distance optical fiber networks.

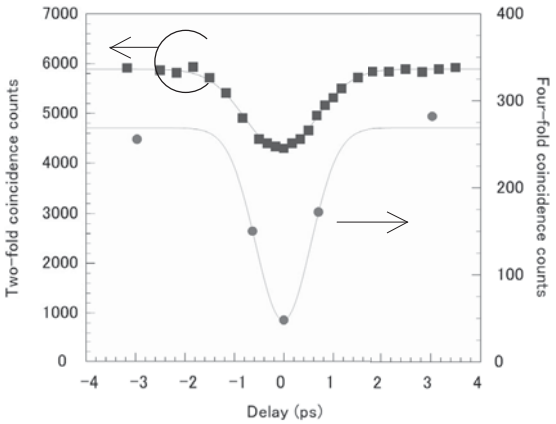

Fig.1 Hong-Ou-Mandel dip by photons from independent photon-pair sources

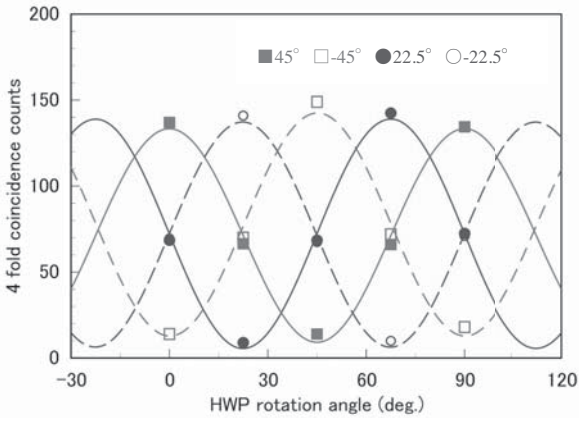

Fig.2 Two-photon interference fringes after the entanglement swapping

Electronic structure calculation of crystal interfaces, adsorbed molecules, and nanostructures

Hiroshi ISHIDA
Theory and Simulation

Recent progress in microfabrication technology has enabled the synthesis of superlattices with atomically controlled layer thicknesses and single molecule transistors. We aim at clarifying the electronic structure of these systems, including the effects of strong Coulomb correlations, by combing first-principles density-functional calculations and many-body techniques like dynamical mean-field theory.

1. Coulomb blockade and Kondo effect in the Hubbard molecules

We considered N-site Hubbard molecules linked between two metal electrodes (Fig.1) and examined their equilibrium electronic structure at temperature T in the zero-bias limit by calculating the finite-temperature Green's function. Here, U denotes the onsite Coulomb repulsion energy, while t_L, t_M, and $t=1$ (chosen as unit of energy) are the hopping integral between the molecule and metal electrodes, that between neighboring sites in metal electrodes, and that between neighboring sites in the molecule, respectively. In the calculation, two semi-infinite electrodes are approximated by finite-size clusters, and the Green's function of the resultant finite system is calculated by applying exact diagonalization.

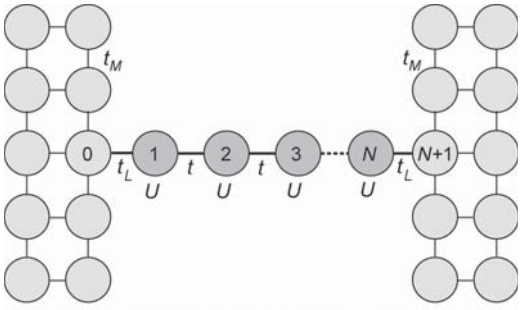

図１：電極間を架橋する単一分子のモデル

As an example, we consider a 3-site chain molecule. Fig. 2 shows its integrated one-electron density of states (DOS) near the chemical potential of metal electrodes, μ, for four temperature values, when μ (alternatively, the gate voltage of the molecule) is varied. While DOS of the non-interacting molecule exhibits three peaks originating from three molecular orbitals, each of them splits into a double-peak structure as a result of the Coulomb blockade. Moreover, the quasi-Coulomb gap of the second molecular orbital is seen to disappear at lower temperatures, indicating the formation the Kondo resonance at μ below the Kondo temperature (*Phys. Rev. B*, 2012). These results demonstrate that the present scheme is capable of describing the electronic structure of adsorbed molecules in the wide parameter range including the ballistic, Coulomb blockade, and Kondo regimes.

図2：鎖分子(N=3)の化学ポテンシャルでの状態密度

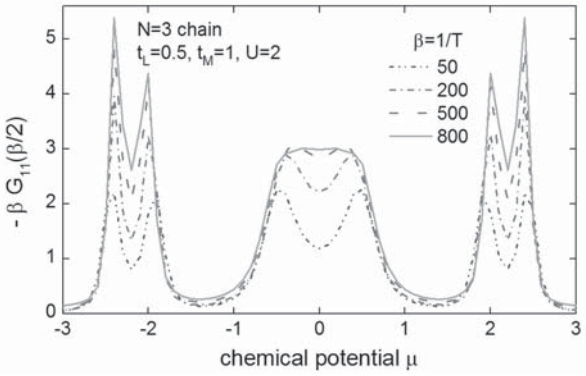

2. First-principles embedded Green's function code including the spin-orbit coupling

We are currently working on implementing the spin-orbit coupling term in our first-principles computer code for calculatng the electronic structure of semi-infinite surfaces and interfaces based on density-functional theory and the embedding tehnique of Inglesfield. Our method will be able to calculate, for example, the electronic structre of topological insulators, especially, the spin-polarized metallic surface states of these materials, more accurately than standard slab calculations.

Ultra High Density Information Recording Materials on Self Assembled Nano-structured Substrates

Akiyoshi ITOH, Arata TSUKAMOTO
Information Storage Group; Supramolecules and Self-Assembly Group

In recent years, much attention has been focused on nano-structured magnetic media for achieving ultra high density recording up to several Tbit/inch^2. Combining self-assembly nano-structured substrates with defined magnetic properties provided by a magnetic film deposited onto the surface, enable a noble approach to create magnetic nanostructure arrays. We tried to prepare and utilize nano-structured substrates such as silica thin film having self-assembled nano-pores and self-assembled silica particle substrate.

The Rapid Thermal Annealing (RTA) of Pt/Cu/Fe multilayered continuous films is effective to obtain perpendicularly magnetized small $L1_0$-FeCuPt grains on thermally oxidized Si substrate. We introduced Rapid Cooling Process into RTA. With the rapid cooling process, growing of grains were prevented, however new shoulder peak in XRD (X-ray diffraction) profile were appeared at slightly lower angle of FeCuPt (002) peak and it might be correspond to the disordered structure of FeCuPt. From electron diffraction patterns and dark field images of single grain by TEM, mostly $L1_0$-ordered polycrystalline structure was observed. Therefore, we preformed additional annealing to above isolated FeCuPt grains by using same annealing chamber of RTA, for crystallizing those poly-crystal grains to form single crystalline grains.

Annealing condition was decided as 600 degree C for 1 hour. The ordering temperature of FePt alloy is ~600 degree C and estimated atomic diffusion length is the order of third nearest neighbor distance in FePt at the annealing condition. From the comparison of the XRD profiles, the intensity of (001) super lattice peak which indicate the formation of $L1_0$-ordered phase is increased, and the shoulder peak at slightly lower angle of (002) is banished as shown in Fig. 1. Thus, FeCuPt grains and are expected to form single crystalline grains. After additional annealing, grains kept almost similar size. Furthermore, we observed crystal structure of a typical single grain after additional annealing by TEM. In most of grains, octagonal symmetric shape is appeared as shown in Fig. 2. From electron beam diffraction measurement of the single grain, series of {110} super lattice and {200} lattice spots are observed with fourfold-symmetry. {110} spots indicate the formation of $L1_0$-ordered structure. Thus, the grain consists of c-axis oriented single crystalline structure from complementary results of XRD covering macroscopic area and localized electron beam diffraction.

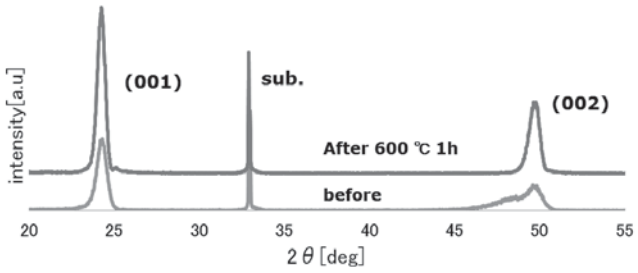

Fig. 1 XRD profiles of before and after the additional annealing

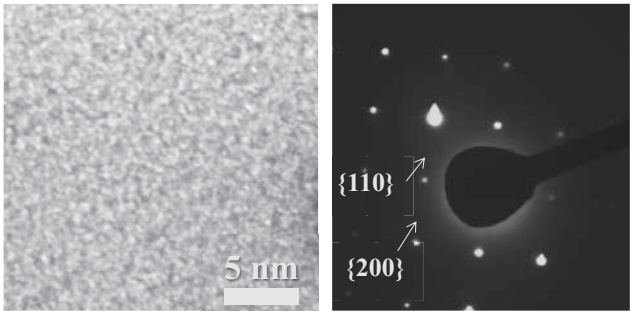

Fig. 2 Bright field image of TEM and Electron diffraction pattern for an isolated grain after additional annealing.

As a result, we found that an application of adequate additional annealing makes grains into $L1_0$ single crystalline structures and grains kept almost similar size.

Pursuing the Limits of Nanomaterial-based Photonic and Quantum Technologies

Nobuyuki IWATA
Nanomaterials and Nanodevices

1. Induced ferromagnetic-ferroelectric multiferroic materials at room temperature

[ABO_3/$REMO_3$](A=Ca,La, B=Fe,Mn, RE=La,Bi, M=Fe,$Fe_{0.8}Mn_{0.2}$) superlattices were deposited on surface treated $SrTiO_3$(100) substrates by pulsed laser deposition method; 3 types of $CaFeO_3$(CFO)-series, 3 types of $CaMnO_3$(CMO)-series, 3 types of $LaMnO_3$(LMO)-series. In a 2θ-θ x-ray diffraction, satellite peaks and Laue oscillations were clearly observed. Those results indicate that the homogenous interface is created. From the results of reciprocal space mapping (RSM), all superlattices except for LMO/$BiFe_{0.8}Mn_{0.2}O_3$(BFMO), cubu-on-cube structure was observed with the film lattice fitted to the substrate lattice in-plain. Sheet resistance of the superlattices showed semiconducting behavior. In the case of CFO-series superlattices, the resistance was too high to measure in our system. Activation energy (E_A) and critical temperature (T_C), where the slope changed, are summarized in Table I. The E_A of CMO and LMO single layer was 0.076 and 0.17eV at higher temperature. The E_A of the superlatatice was smaller than the value of single layers, indicating that the electron transfer, intermixing of cation at the interface, and modification of the band structure. At the T_C, magnetic transition is expected. The author did the organizer at the biggest joint symposium in this field (JSAP-MRS 2012 Spring Meeting). The author was invited to the OMTAT international conference hold at Kochi, India with the title of Oxides heterostructures for giant magnetoelectric effect.

Table I : Summary of activation energy (E_A) and critical temperature (T_C) of superlattices.

	$REMO_3$	$LaFeO_3$(LFO)		$BiFeO_3$(BFO)		$BiFe_{0.8}Mn_{0.2}O_3$ (BFMO)	
ABO_3	Temp. region	Lower Temp.	Higher Temp.	Lower Temp.	Higher Temp.	Lower Temp.	Higher Temp.
CMO (0.076eV)	E_A(eV)	0.082	0.050	0,034	0.030	0.013	0.19
	T_C(K)	151.1		125.6		71.2	
LMO (0.17eV)	E_A(eV)	0.55	0.16	---	---	---	0.12
	T_C(K)	240.7		---		---	

2. Single-Walled Carbon Nanotube (SWNT)

In order to develop a FET property using just one SWNT, substrate heater was redesigned. Approximately 30 of G/D ratio, which indicates the quality of SWNTs, was extremely improved to be over 400. Possible reasons are as follows; carbon source is fully reactive state for introduction to catalysts, redox catalysts surface is obtained just before CVD deposition, and optimized CVD condition depending on the catalysts diameter is realized. The value of G/D ratio was less than 50, 50~100, and over 100 in SWNT with a diameter of 1.1 nm, 1.46 nm, and 1.65 nm, respectively. There was a relationship between catalysts diameter and CVD condition, in particular heater temperature, gas pressure, and flow rate of carbon source. In addition, we found that the chirality was controllable by free electron laser (FEL) irradiation after start of CVD deposition.

Preparation of Metallic Clusters in Solution and Applications to Catalysis

Ken JUDAI
Nanomaterials and Nanodevices

Metallic clusters, which are defined as aggregation compounds of several or hundreds atoms, have been usually produced in the gas phase. The number of atoms is critical function to describe the properties of clusters, and the difference of only single atom can cause remarkably changing for reactivity and stability of the clusters. This indicates that the atomically precise control of cluster size becomes important for the material applications. In this work, gold clusters, the most stable metal element for air-oxidation, were prepared in solution phase, and were size-separated. The electrochemical measurement was also attempted to the gold clusters for catalytic application.

1. Preparation of gold clusters in solution and size separation

The problem on the cluster production with a vacuum chamber in the gas phase is extremely low yield. Thus, metallic clusters with ligand molecules were prepared in solution and were size-separated by chemical technique. In detail, tetrachloroauric(III) acid under the presence of phenyl ethane thiol was reacted with reducing agent. The gold clusters protected by thiol were obtained. The size exclusion chromatograms are shown for sampling at the periods of 1, 3, 7, 24 hours after the addition of borane reducing agent. Although the chromatogram at 1 hour has many peaks to be regarded as reaction intermediates, the other chromatograms indicate the termination of chemical reactions. It should be noted that the peak at 50 min retention time has been changing during 24 hours. The cluster size might change in this time scale.

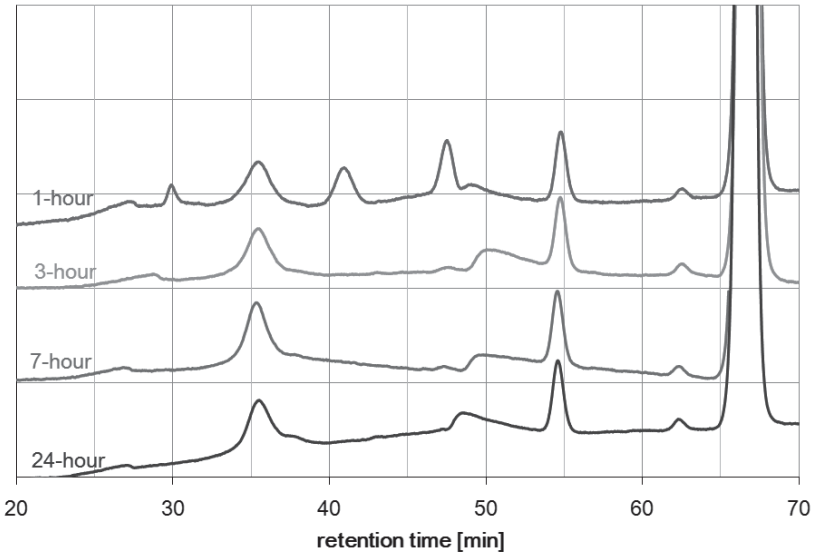

2. Electrochemical measurement for catalysis application

The most stable gold clusters can be isolated by producing condition and careful choice of extraction solvent. The gold cluster was reduced by sodium borohydride and was extracted with acetonitrile. The gold cluster protected by phenyl ethane thiol, $Au_{25}(SR)_{18}$, was obtained. The resulted cluster was casted on the surface of glassy carbon electrode. The cyclic voltammetry measurement has been done in sulfuric acid solution. The different potentials to gold bulk surface were observed. The catalytic activity will be examined by this technique for clusters on the surface.

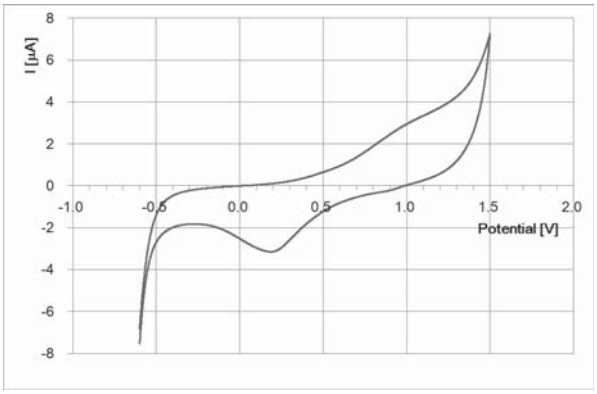

Actin Cytoskelton Dynamics Control Adipocyte Differentiation Via Regulation of MKL1

Koichiro KANO
Medical Group

The hallmark of adipogenesis process is the dramatic alteration in actin cytoskelton as the structure of filamentous actin is converted from stress fibers to cortical actin. Here, we report that actin cytoskelton dynamics act as a trigger of adipocyte differentiation. Actin cytoskelton remodeling was immediately caused via the down-regulation of RhoA/ROCK signaling, which is a prominent regulator of cytoskeletal dynamics, and this actin remodeling was required for a master regulator PPARγ expression and adipocyte differentiation. Also it was found that the cellular G-actin levels were rapidly elevated depending on adipocyte differentiation, and increasing G-actin caused adipogenesis by preventing nuclear translocation of MKL1, which is a transcriptional co-activator. Moreover, we revealed that MKL1 expression was reduced during adipogenesis, and further only knockdown of MKL1 could trigger adipocyte differentiation. Besides, PPARγ was closely involved in the down-regulation of MKL1 in a positive feedback manner. Our findings provide new insights to the regulatory mechanism of adipocyte differentiation that actin cytoskelton dynamics control adipocyte differentiation via regulation of MKL1, and that MKL1 is a novel repressive regulator of adipocyte differentiation.

Anti-tumor Effect of Inhibition *LIT1* Gene Transcription by using as New Therapeutic Agent

Tsugumichi KOSHINAGA
Medical Group(Pediatric Surgery, School of Medicine)

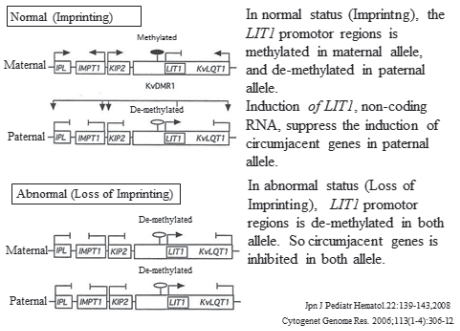

Beckwith-Wiedemann syndrome (BWS) is a human imprinting disorder with a variable phenotype. The major features are omphalocele, pre- and postnatal overgrowth, and macroglossia. BWS predisposes patients to embryonal tumor (Wilm's tumor, Hepatoblastomoa) in 5~10% degrees of patients.BWS is associated with epigenetic alterations in two imprinting control region, KvDMR and H19DMR, on chromosome 11p15.5. The absence of methylation in KvDMR is called loss of imprinting(LOI) and leads to overexpression of *LIT1* gene. This gene down-regulates circumjacent genes including $p57^{KIP2}$, tumor suppressor gene. We investigate the association between overexpression of *LIT1* gene and tumorigenesis in BWS. LOI in KvDMR reported to happen in several adult tumors.

On the other hands, PYRROLE-IMIDAZOLE POLYAMIDE(PIP) polyamide can recognize a specific DNA sequence and bind the minor groove of double strand DNA. If PI polyamide is designed against a sequence of the target transcription factor binding site, it might artificially down-regulate the expression of a target gene. We generated PIP binding to promoter region of *LIT1* gene to investigate anti-tumor effect.

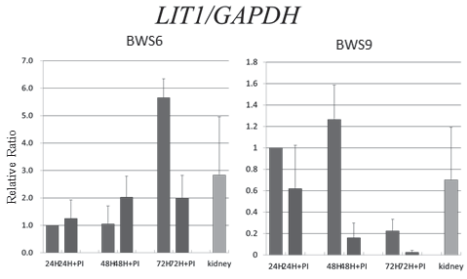

We co-cultured PIP(h-CCAAT1;PI-1, h-CCAAT3;PI-3) with human BWS fibroblast cell line(BWS6,9). In the same manner, we administered PI-1,PI-3 to Hepatoblastoma cell line(HuH6 clone5, HepG2), and Wilm's tumor cell line(G401). These tumor cell lines showed de-methylation status in *LIT1* promotor region, they may happen LOI in KvDMR.

After 72hours co-cultured, BWS6,9 significantly showed the down-regulation of *LIT1* expression ($p<0.05$), compared with untreated cell analyzed by real-time RT-PCR. And, G401 significantly showed difference the number of alive cells by using WST-8 procedure after 120 hours co-cultured. G401 also showed the down-regulation of *LIT1* expression($p<0.05$) compared with untreated cell.

These data suggest that PIP which suppresses LIT1 expression have anti-tumor effect to tumor with LOI in KvDMR. This PIP may have possibility to be new therapeutic agents. Now, we investigate anti-tumor effect of this PIP using G401 xenograft model mice in vivo. If PIP contracts tumor size in vivo, this PIP thought to contribute to development of drug discovery.

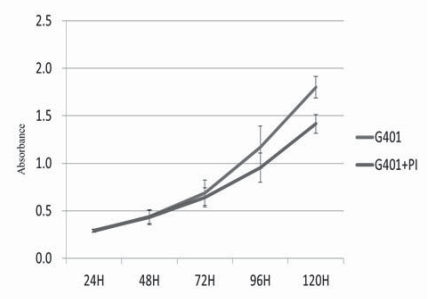

Experimental Studies for Quantum Memory using Neutral Atoms

Takeshi KUWAMOTO
Quantum Information Group

As a next-generation information, communication and computer technology, quantum information processing is hoped very much. In order to construct scalable quantum processing system, quantum memory is indispensable. Our aim in this project is establishing the basic technique for materializing the quantum memory. We especially intend to store the quantum entangled states in neutral atoms.

1. Study for storage of orthogonally entangled photon pairs

Last year, we improved the generation system of orthogonally polarized photon pairs, which are light source when creating the polarized quantum entangled states in the future. In this year, we pushed forward to store the photon pairs into rubidium (Rb) atoms enclosed in a glass cell.

We utilize the electromagnetically induced transparency (EIT) to store the photon pairs in atoms. The photon pairs, which are generated with nonlinear optical crystal, typically have several-hundred-GHz frequency expansion. To store the photon pairs, this wide frequency expansion must be extremely narrowed, because the effective bandwidth of EIT is several MHz. We used two etalons with different free spectral range for frequency-narrowing the photon pairs. The expected bandwidth of photon pairs passed thorough them was about 300 MHz.

To verify the bandwidth of photons passed through two etalons, we observed the absorption of photons by Rb vapor at various temperatures. FWHM of absorption spectrum of Rb atoms is typically about 500 MHz. Figure 1 shows the absorption rate of the photon pairs as a function of Rb vapor temperature. At vapor temperature of 95℃, 97% of photons was absorbed into Rb vapor. This means that the photon pairs with several-GHz bandwidth could be frequency-narrowed by two etalons until 500 MHz level.

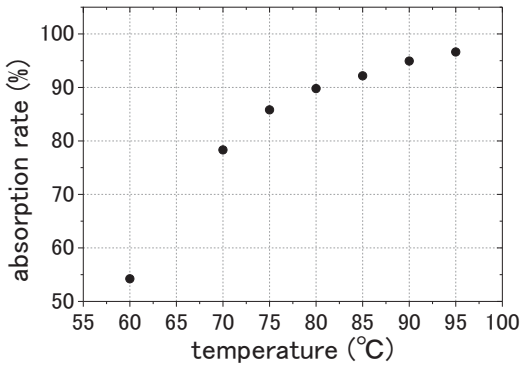

Fig. 1 Absorption rate of frequency-narrowed orthogonally polarized photon pairs by Rb vapor as a function of the temperature of vapor.

We now perform experiments that observe the orthogonally polarized photon pairs passing through the Rb vapor by EIT effects. Since the transmitted photon pairs have only few-MHz frequency width, they are suitable quantum correlated photon source for storage in Rb atoms. In future, we will perform two-photon interference measurements of EIT-transmitted photons, storage of orthogonally polarized photons in Rb atoms, generation of orthogonally quantum entangled states with orthogonally polarized photon pairs, and storage of quantum entangled states in atoms.

2. Improvements of coherent light storage system

We improved the coherent-light-storage experimental system for increasing the storage efficiency of laser light in Rb vapor. Last year, we achieved the storage efficiency of 60% at storage time of 5μs. As a result of various improvements such as optimization of laser power, its frequency, and Rb cell temperature, the storage efficiency of laser light was increased to 85% at storage time of 5μs (Fig. 2).

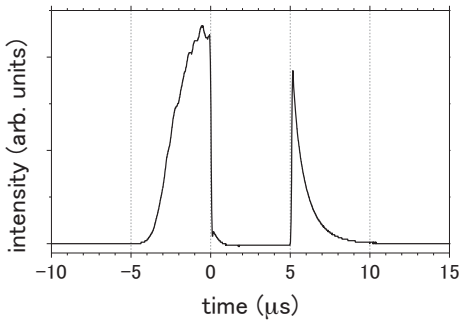

Fig. 2 Storage of laser light resonant with Rb atom.

Construction of the Escherichia Coli Expression System of the Cell Membrane Permeable iPSCs Induced Factors That Strengthened Proteolysis Resistance

Yoshikazu MASUHIRO
Medical Group (Department of Applied Biological Sciences, College of Bioresource Sciences)

It is required that the induced pluripotent stem cells (iPSCs) to use for regenerative medicine are safe hereditarily. As for the current iPSCs derivative method, the virus method is mainstream, but gene variation is concerned about by this method. Therefore, the derivative method using protein and the reagent is expected in future. The derivative method with the cell membrane permeable proteins have been already reported by two groups, but induced efficiency is extremely bad, and there are many problems (operation and preparations are great). For this reason, it is thought that cell-permeable proteins are degraded in a cell early. Therefore, in this study, we work on development of iPSCs induced factor (Oct4, Sox2, Klf4, Glis1) having resistance in the proteolysis in the cell. We try in particular application (it fuses as a tag) of proteolysis-resistant motif Stabilon which we developed originally in our laboratory. From a past study, because the Stabilon was effective about Sox2 and Glis1, we made Stabilon fusion and a non-fusion for these proteins. From the quantity of the expression and simplicity of purification, we decided that these proteins expressed in Escherichia coli as an inclusion body. We performed cloning of these factors in pET28a expression plasmid and produced it in BL21(DE3). Oct4; 3mg, Sox2; 3mg, Sox2-Stabilon; 3 mg, Klf4; 4.5mg, Glis1; 1.2mg and Glis1-Stabilon; 1.2 mg expressed in BL21(DE3) per 1 liter LB culture media. In addition, we purified these proteins under guanidine hydrochloric acid and urea (denature condition) from an inclusion body, and performed refolding by the dialysis. These denature proteins refolded about Oct4; 30%, Sox2; 10%, Sox2-Stabilon; 30%, Klf4; 5%, Glis1; 0% and Glis1-Stabilon; 5%. In addition, we were able to confirm the DNA binding capacity by Gel shift assay about Sox2, Sox2-Stabilon. We examine these transcription activity and we introduce it into mouse MEF cell and examine the induced efficiency of iPSCs in future.

Pharmacokinetic/Pharmacodynamic Analysis of Tumor-localizing Photosensitizing Compounds

Takahiko AOYAMA, Yoshiaki MATSUMOTO
Medical Group(College of Pharmacy)

To describe the relationships between effects following photodynamic therapy, light dose, and plasma compound concentration, we investigate the pharmacokinetics of novel compound CT101019a (Fig. 1).

1. Pharmacokinetics of CT101019a

To characterize the pharmacokinetics of CT101019a after intravenous administration at various doses in rats, dose linearity of CT101019a was observed. The plasma concentration-time profiles were analyzed by a non-compartmental method. The analysis of dose linearity was performed for AUC using the power model. CT101019a showed nonlinear pharmacokinetics in rats.

2. Development of Pharmacokinetic model predicting human pharmacokinetics for Talaporfin

We develop the pharmacokinetic model of talaporfin (Fig. 2) predicting human pharmacokinetics using rat, mice and human data. The pharmacokinetic differences among species were modeled by allometric scaling method. The prediction of rat and human pharmacokinetics had a bias (Fig. 3). Accordingly, we optimize the model incorporating the physiological parameters such as rate of bile excretion, hepatic blood flow and plasma volume.

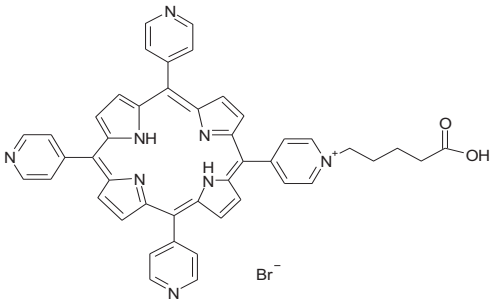

Fig. 1. Chemical structure of CT101019a.

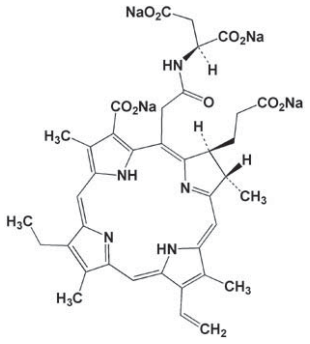

Fig. 2 Chemical structure of talaporfin.

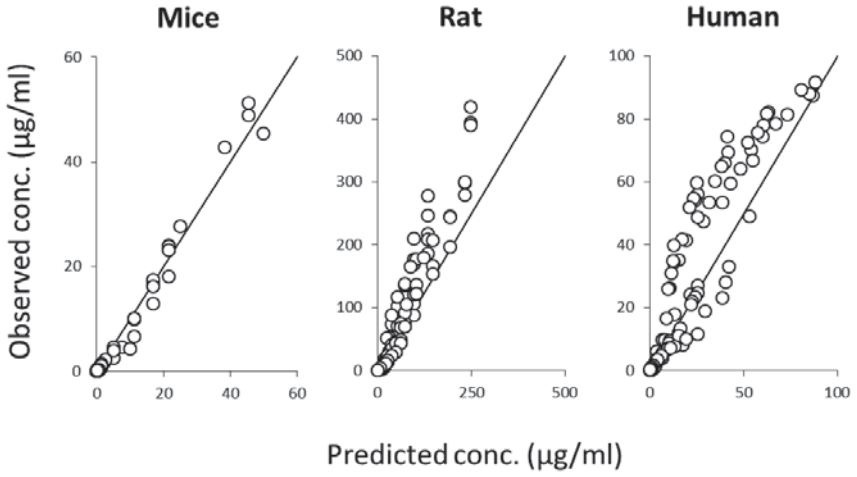

Fig. 3. Goodness-of-fit plots for pharmacokinetic model of talaporfin.

Self-assembly and Self-organization from the viewpoint of Device-fabrication Methods

Sachiko MATSUSHITA
Supramolecular and Self-Assembly; Energy Technology

Two subjects related with self-assembly and self-organization were studied with perspective of the developments of unexplored scientific fields and new technology: 1) Dye-sensitized photonic crystal electrodes, and 2) Fabrication of optical devices via self-assembly.

1. Dye-sensitized photonic crystal electrodes

There are few reports on photoelectric conversion efficiency using naturally-occurring dyes for dye-sensitized solar cells (DSSC). This is because the matching with an excited electronic level of naturally-occurring dye to the conduction band of semiconductor is problematic; the excited electrons are easily relaxed to the steady state with fluorescence or heat emission. We examined the fluorescence inhibition effect of a self-assembled photonic crystal using Chlorine e6 dye. Chlorine e6 is derived from chlorophyll and has a long excited electron lifetime.

We prepared TiO_2 inverse opals with various particle sizes by liquid phase deposition (LPD) and described their effect on DSSCs with regard to structural, optical and electrochemical properties. In addition, we explored the implications of fluorescence lifetime measurements relative to the photonic band diagram and the amount of adsorbed dye. After these precise experiments, it is possible that the photonic band influenced the internal quantum efficiency per one dye molecule.

A detailed verification of this assumption cannot be performed for a self-assembled photonic crystal with many defects. Such verification would require a dye sensitizing electrode with a full/complete photonic bandgap. To prepare such electrochemical photonic crystal, we also performed the calculation [1] and fabrication of a photonic crystal structure of (001) rutile TiO_2 substrate by deep reactive ion etching (RIE) using SF_6 plasma [2]. The IR spectrum of this fabricated photonic structure was compared with the photonic band diagram.

2. Noble Planar and Symmetric Nanostructures in Prospective Plasmonic Devices

Noble planar and symmetric nanostructures, such as rod or spiny structures, were prepared by the combination of colloidal self-assembly, thermal sintering and chemical etching, which enables the tuning of both size of the particle and neck diameter. As a result, we could fabricate nanostructures on that six nanorods and tips are arrayed in a planar arrangement on a spherical particle. Localized surface plasmon resonance was observed from each structure [3]. To evaluate the sensing ability of structures, SERS was measured. The rod structure showed the biggest SERS effect among our structures in spite of the smallest amount of Au coating.

[1] S. Matsushita, O. Suavet, H. Hashiba, Electrochim. Acta, 55 (2010) 2398-2403.
[2] A. Matsutani, M. Hayashi, Y. Morii, K. Nishioka, T. Isobe, A. Nakajima, S. Matsushita , Jpn. J. Appl. Physics, 51 (2012) 098002.
[3] T. Miyamoto, S. Saito, T. Isobe, A. Nakajima, S. Matsushita, Chem. Commun., 48 (2012) 1668.

Applied Chemical Biology: Strategy to Cure Cancer Patients

Takayoshi WATANABE, Hiroki NAGASE
Medical Group (Chiba Cancer Center Institute)

Exploiting an enormous amount of potentials of organic chemistry, we have conducted chemical biological approaches to cure cancer patients. Following two distinct but important approaches have been studied for the last four years and found promising preliminary results. The first one is DNA binding molecule of PI polyamide for cancer therapy and the second is a novel chemosensitizing radiation therapy.

1. PI polyamides targeting cancer related genes for anti-cancer therapy

Pyrrole-Imidazole (PI) polyamide molecule was originally designed from structures of natural DNA binding molecule, such as Distamicine and Diocarbamicine and has been discovered as a synthetic molecule which recognizes the minor groove of Watson-Click base pairs of double-stranded DNA in a sequence-dependent manner. We have developed a semi-automatic synthesis system for PI polyamide, which are able to regulate specific target gene-expression under specific transcription factor binding inhibition for biological functional studies and perhaps patient therapy. PI polyamide immediately penetrated the nucleus *in vitro* and *in vivo* without any vehicle. After intra venous injection it rapidly reduce the serum concentration, delivered to most of tissue cells, excreted to urine or bile juice and did not metabolize in animals. The PI polyamides, designed for anti-Tgfb1 and anti-MMP9 activity, were well tolerated, reduced target gene expression and showed therapeutic effects in animal models of human diseases. For instance, after I.V. administration of anti-MMP9 polyamides, tumor metastasis was significantly suppressed in the mouse model of human liver metastasis of colon cancer. This new auto-synthetic chemicals can be designed for many transcriptional regulation of transcripts and applied to prove many biological hypothesis of transcriptional regulation for cancer research, and may be used for cancer therapy in the future.

2. A novel chemosensitizing radiation therapy by using synthetic porphyrin derivatives

Photodynamic therapy (PDT) is a medical treatment that uses a photosensitizing chemical and a light source (long wave length light can reach around 1cm depth of human tissues) to activate the applied chemical. The result is an activated oxygen molecule that can destroy nearby cells. Precancerous cells and certain types of cancer cells can be treated by PDT. Cancer cells uptake more of the porphyrin derivatives and retain the chemicals in a long duration. Thus, the PDT can introduce a cancer cell specific therapy. We invented the radiation-sensitizing chemical of the porphyrin derivatives, which can be used for PDT and may also induce photon activation therapy (PAT), provoking the emission of Auger electrons after inducing a photoelectric effect. X-ray radiation allows for the treatment of cancers that are deep inside the human body. We observed an induced cancer cell death after irradiation following administration of the porphyrin derivative. This study orchestrated harmony of works among medical school, school of pharmacy and college of science and technology.

Research for High Density and High Speed Magnetic Recording
- Thermally Assisted Magnetic Recording Applying Near Field Optical Light -

Katsuji NAKAGAWA
Information (Storage) Group

It is a challenging issue to write magnetic domains on a stable magnetic recording layer for the future high density magnetic recording technology, because the stable magnetic recording layer for high density recording is extremely sustainable not only against thermal agitation but also against recording magnetic field. We study thermally assisted magnetic recording that can enable to write nano-meter size magnetic domains on stable magnetic film by the technique that applies the confined laser light by a near field optical method. The research has been collaborated with Assistant Prof. Ashizawa. The structure of surface plasmon antennas is designed by optical and thermal simulation collaborated with Associate Prof. Ohnuki. Magnetic films and fabrication e-beam lithography processes for surface plasmon antenna are also prepared. We have also started femto-second laser pulse recording collaborated with Associate Prof. A. Tsukamoto and Prof. A. Itoh.

1. Thermally assisted magnetic record applying femto-second laser with surface plasmon antenna

To study thermally assisted magnetic recording focusing on surface plasmon effect as well as thermal diffusion effect, a 90-femto-second laser pulse impinged upon surface plasmon antennas on $Co_{55}Pt_{30}Cr_{15}$–SiO_2 granular film. It is important to use a femto-second laser pulse to analyze those effects, because the effects can be degraded by the thermal diffusion during the laser pulse duration if a longer laser pulse is applied. A SiN dielectric inter-layer was fabricated to keep an accurate distance between the antennas and the granular film. Written magnetic domains caused by surface plasmon effect were clearly observed by a magnetic force microscope. The minimum domain corresponded to 166 nm × 120 nm in size even though the laser spot diameter was about 50 μm. The surface plasmon effect was evaluated by the Finite-Difference Time-Domain method, and the thermal diffusion effect was also calculated to study thermally assisted magnetic recording.

2. Combination of dielectric waveguide and surface plasmon polariton

It is very important how to locate surface plasmon antennas in magnetic head for thermally assisted magnetic recording. We studied the dependence on energy transfer efficiency to get high efficiency. One of the methods that surface plasmon antennas are placed along with a waveguide was investigated by simulation. It is revealed that a confined circularly polarized light can be created by this method.

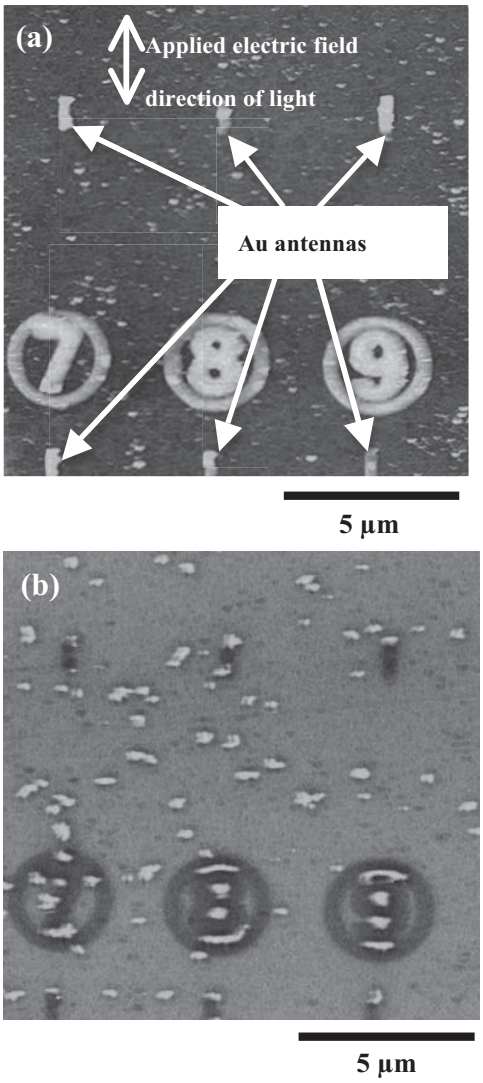

Fig. 1 The surface morphology (a) and the magnetic domains (b) after a 90 fs laser pulse train was exposed over the entire surface of the $Co_{55}Pt_{30}Cr_{15}$ – SiO_2 granular film. The applied Au plasmon antennas were 35 nm in thickness, and their width and length were nearly 100 nm and 1 μm, respectively.

Development of Photonic to Chemical Energies Transformation Systems

Nobuyuki NISHIMIYA
Energy Technology

Several processes that transform photonic energy to chemical energies such as hydrogen energy have been studied through separation and recovery of hydrogen by means of hydrogen occluding alloys from low purity hydrogen produced by microorganisms on photosynthetic reactions and from hydrogen mixtures produced by hydrogen fermentation as well as through designing and preparation of hydrogen occluding composites imparted with photocatalytic activities. Specification of the active entities of hydrogen fermentation of practically employable microorganism mixtures established at the Tanisho Laboratory of Yokohama National University and enhancement of hydrogen storage by nano-sized layer compounds composed of boron, carbon and/or nitrogen have been concentrated.

1. Specification of microorganisms of hydrogen fermentation

Hydrogen fermentation by the well-selected microorganism mixture established at the Tanisho Laboratory of Yokohama National University was permitted to evolve 1 L STP of hydrogen an hour, and the entity of the hydrogen fermentation was analyzed to specify the identification of the microorganisms. Conventional procedures are apt to fail to specify the very active entities due to the possibly poor growth rate of the essential microorganisms. An improved procedure was thus employed comprising abstract of DNA from the well-selected microorganism mixture, enhancement of 16S rDNA by PCR (Polymerase Chain Reaction), separation of the specified 16S rDNA by DGGE (Denaturing Gradient Gel Electrophoresis) and reading the arrangement of DNA bases. Several microorganism species have been identified based upon DDBJ (Japanese database on DNA).

2. Separation and recovery of bio-hydrogen by magnesium-based alloys

Additional use of soft sol-gel encapsulated Mg-10%Ni/NbF_5 composite was attempted and hydrogen recovery from Spirulina vial was performed by much less amount of the hydrogen occlusion material. While the amount of the material was reduced by half, the encapsulation was not complete as detected by a detectable reaction of Mg with water. Completion of the encapsulation and further reduction of the weight are to be attained.

3. Hydrogen storage by graphene-derived carbon nano-balls

Carbon nano-balls were prepared by separation of graphene sheets from graphite as proposed by Hummers, agglomeration of oxidized graphene sheets around metallic cores and reduction of ball-like agglomerates under hydrogen. Larger amounts of hydrogen were adsorbed on surfaces inside the mesopores of the nano-balls than those on even graphitic surfaces.

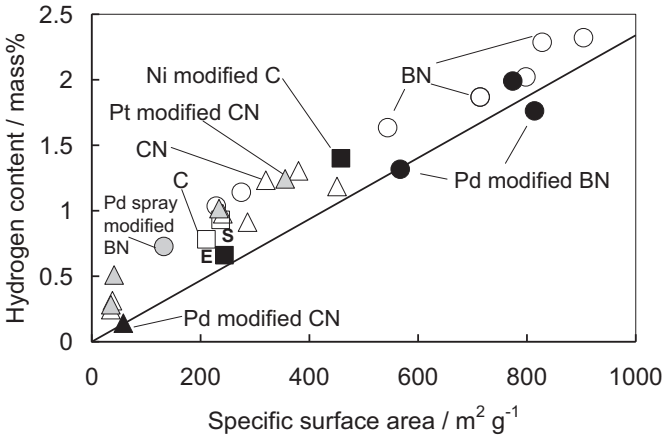

Figure 1. Variation of hydrogen storage capacity at 77 K and 0.8 MPa with specific surface area

4. Hydrogen storage by nano-sized layer compounds composed of boron, carbon and/or nitrogen

Among the B-C-N phases that do not contain substantial amounts of rare metals, BN and C_3N_4 (CN in Figure 1) were found promising as positively deviated from the theoretical line in Figure 1.

Nano-Electromagnetic Simulation and Its Applications to Plasmonic Devices

Shinichiro OHNUKI
Quantum Theory and Computation Group

This work aims at developing fast and reliable electromagnetic simulation methods for studying interaction between light and nanoscale objects. We apply our computational methods to designing nanoscale devices through the collaboration with researchers of the *N*. research project.

1. Design of Plasmonic Antennas with Particulate Media for All Optical Magnetic Recording

We have designed plasmonic antennas to generate the localized circularly polarized light inside the bit-patterned media for realizing ultra-high density magnetic recording. Using the ADE-FDTD method, the generation time and intensity of the localized circularly polarized light are clarified in terms of the combination of antennas.

2. Time Domain Responses of Electromagnetic Fields by Integral Equation Methods

We have developed novel fast and accurate solvers based on integral equation methods with fast inverse Laplace transform for time domain electromagnetic problems. The advantages of our proposed method are (1) the computational error is easy to be controlled, (2) there is the no restriction of selecting time step size, and (3) an arbitrary observation time can be selected. Using our proposed method, we analyze time domain responses of electromagnetic fields near nanoscale antennas and dipole moments of molecular motors.

3. Multiphysics Simulation of a Nanoplate in Laser Fields

A nanoplate in laser fields has been analyzed by the coupled Maxwell-Schrödinger scheme which is based upon the FDTD method. We have investigated the current densities and electromagnetic fields near the nanoplate in terms of tunneling effects due to well structures. Advantages of our proposed method are clarified in comparison with conventional classical solvers.

4. Modeling of Plasmonic Waveguides for a High Sensitivity Optical Sensor

We have proposed an optical sensor which consists of a metal stripe and nano wire inside an optical fiber. Using the proposed device, electromagnetic energy is concentrated around the metal stripe and the energy can be efficiently absorbed into the nano wire. We verity that the electromagnetic energy inside the nano wire becomes three times larger than that for the case without the plasmonic waveguide.

5. High-Precision Analysis of Electromagnetic Scattering Problems

To obtain reference solutions for electromagnetic canonical problems, we have developed a mode matching method. The method has been proposed for a dielectric sphere with a metal shell as an example of 3D canonical geometries. Scattered electromagnetic fields are analyzed and computational error is confirmed.

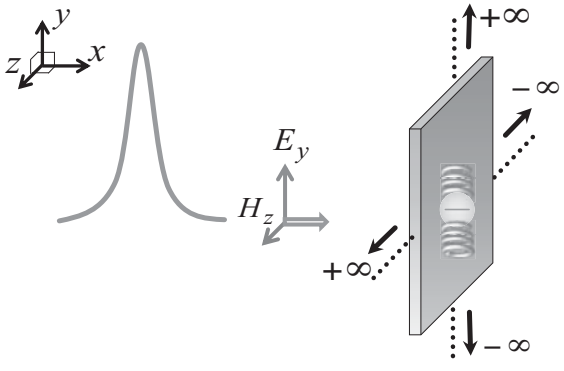

Figure 1 Coordinate systems of the nanoplate.

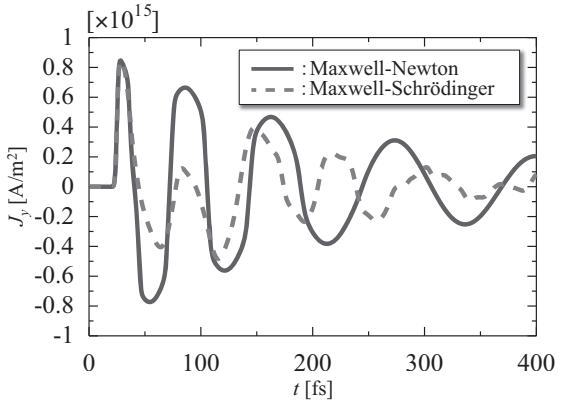

Figure 2 Time response of the current density.

Self-Assembled Supramolecules and Their Applications to Energy, Medical, and Information Technologies

Joe OTSUKI
Supramolecular and Self-Assembly Group; Energy Technology Group

Self-assembly of appropriately designed molecules will afford a bottom-up method for producing nanostructures. This work aims at developing new molecular self-assembling systems, revealing self-assembled structures and dynamic behaviors at the molecular level, and searching for applications of self-assembly to energy, medical, and information technologies through the collaboration with researchers of the *N*. research project.

1. Self-Assembly of Molecules and Quantum Dots

The low-density solar radiation is efficiently collected by light-harvesting antenna made of self-assembled chlorophyll molecules, where highly-efficient excited energy transfer processes take place. Such structures, if we could construct by design, would be used in artificial photosynthetic systems and organic photovoltaics. We have found that pyridine-appended chlorophyll molecules form double helical structures, which was revealed by the single crystal X-ray crystallography, reminiscent of the double helices of DNA (Figure 1). While an oxazole-appended chlorophyll derivative leads to a stair-case type architecture. These works constitute a step toward constructing artificial antenna systems based on molecular assemblies.

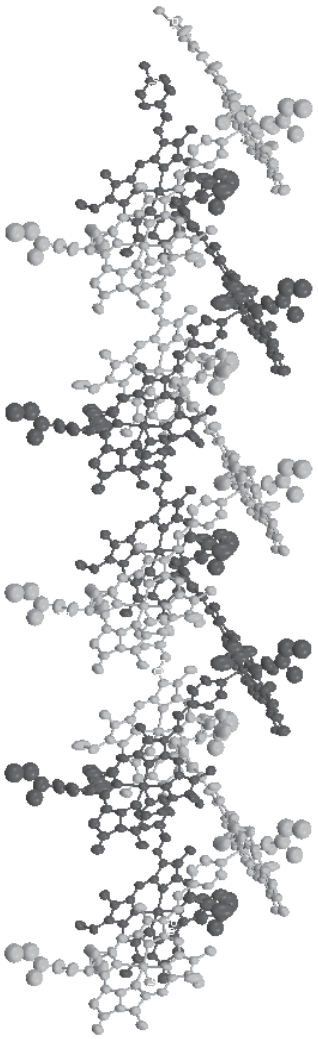

Figure 1. Double helix formed by a chlorophyll derivative.

In the field of molecular assembly, we revealed the arrangement and behaviors of a double-decker type porphyrin complex on a substrate surface at the molecular scale [*J. Nanosci. Nanotechnol.* **2012**, *12*, 159].

We are also working on the preparation of quantum dots, entrapment of the quantum dots in silica coatings, and fabrication of ordered assemblies of the silica-coated quantum dots. The series of techniques will be used in devices for quantum cryptography. Coating with silica without deteriorating the high quantum yield of emission of quantum dots is the bottleneck at present, which is the main focus of our ongoing work.

2. New Dyes for Dye-Sensitized Solar Cells

We have prepared new dyes based on donor-substituted perylene dicarboxylic derivatives, in which the donors, the side arms, and the adsorption sites to the TiO_2 electrode were varied. No new dyes, however, exceeded previously reported our record of 3.1%. Some new ruthenium-based complexes were also prepared and their structures and properties were revealed.

In relation to photovoltaics, we studied some aspects of graphene oxide, which is a promising substitute for widely used ITO electrode. We successfully prepared reduced graphene oxide thin films with good electrical properties under heat treatment with temperature lower than reported [*Appl. Surf. Sci.* **2012**, *259*, 460; *Appl. Nanosci.* **2012**, DOI 10.1007/s13204-012-0144-2].

Comparison of the structure of conjugate Fermi holes in He-like systems and artificial atoms

Tokuei SAKO
Quantum Theory and Computation group

Controlling electronic properties of nanomaterials requires our deep understanding in the behavior of electrons confined in nano-scale objects. Through the continuing research of this *N.* project we have found last year the existence of the so-called *conjugate Fermi hole* in the wave function of two electrons with antiparallel spins. This year we have focused on artificial atoms or quantum dots and have examined in detail the structure of conjugate Fermi holes in the systems. As a consequence of the analysis, the origin of the first Hund rule in artificial atoms has been rationalized, and the difference in the mechanism operating in artificial atoms and in the corresponding He-like systems has been clarified.

Empirically derived Hund's rules of the pre-quantum-mechanics era predict the ordering of the energy levels possessing different spin and orbital angular momentum quantum numbers. They have proved to be almost universally valid for atoms, molecules, and quantum dots. Yet, despite of a long standing debate the search for their origin persists, primarily due to the lack of the precise knowledge of the electronic structure in different spin states. We explore the origin of the first Hund rule for a two-dimensional model of He-like systems and that of two-electron quantum dots. They represent ideal systems providing a direct fundamental insight into the structure of the internal part of the fully-correlated wave functions, allowing an unambiguous argument. An examination of their probability density distributions reveals indeed the existence of a region in the internal space which we refer to as a conjugate Fermi hole. In this region the singlet wave function has a smaller probability density than the corresponding triplet one, in contrast to the genuine Fermi hole where the triplet has a smaller density than the singlet. Due to the presence of this conjugate Fermi hole the singlet probability density has to migrate far away from the center of the one-electron potential. This rationalizes the well-known broader electron density distribution of the singlet state relative to the corresponding triplet. This key observation explains the singlet-triplet energy gap.

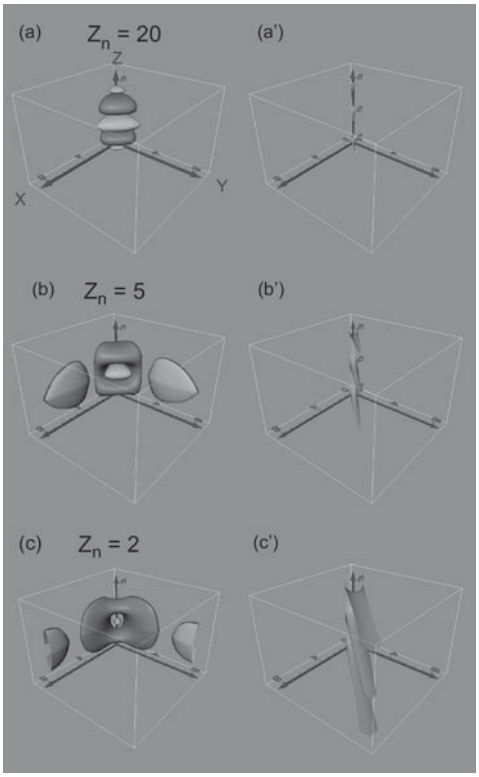

Structure of the genuine and conjugate Fermi holes in the internal space for the (1s)(2p) singlet-triplet pair of states of He-like systems: (a) – (c) correspond to the nuclear charge Z_n of 20, 5, and 2, respectively. (a') – (c') represent the electron repulsion potential for the corresponding Z_n.

The results of this study has been published as an regular article in Journal of Physics B, which has been selected as an IOP Select paper for its "significant breakthrough and high impact" [1]. Moreover, this content of this paper will be covered by Europhysics News of its January issue in 2013 [2].

[1] T. Sako et al., J. Phys. B, **2012**, 45, 235001(13 pages).
[2] T. Sako et al., Europhysics News, to appear in January issue (2013).

Synthesis of Nano-rod Devices with Wide Band Gap Semiconductor Effect

Kaoru SUZUKI
Nanomaterials and Nanodevices Group

My research aims at fabrication of nano-materials and nano-devices for high functional applications such as nano-tube sensor, nano-rod transistor and wide band gap semiconductor nano-film for water-splitting by using fundamental techniques of nano-process and fabrication of nano-materials. Using the achievement of the investigation, progress of energy conversion system, information technology and biotechnology can be expected.

1. Metal encapsulated carbon nanotube for magnetic force microscope probes

We have synthesized directly ferromagnetic metal (Ni) and composition metal encapsulated carbon nanotubes (CNTs) for probe of magnetic force microscope or spin device on a mesh grid for viewing transmission electron microscope (TEM) by pyrolysis of ethanol solution. These metals inside CNTs identified Ni and SUS with energy dispersive X-ray (EDX) spectrum analysis. The diameter and length of the metal core is in the range of 10 – 80 nm and 100 – 800 nm with varying heating period and temperature, respectively. The walls consist of cylindrical graphene sheets with 3 -50 layer.

2. Creation of carbon nano-tube/fiber and diamond-like carbon circuit

We have synthesized phosphorus doped n-type carbon nano-tube/fiber by Joule heating on ethanol/Si surface, and diamond-like carbon films by ion beam plating method. Type of p-n junction diode and wiring were created by focused Ga+ ion beam injection.

3. Synthesize of photocatalytic SrxLa1-xTiO3 film for hydrogen generation on polymer films with visible area in solar light excitation by laser induced forward transfer method

La doped TiO2 have attracted great interest for photocatalytic properties, which can be used visible area in solar light although only TiO2 limiting with ultra violet area. We have successfully crystallized perovskite structure films which were La doped TiO2 thin film of La2Ti2O7, Sr doped TiO2 thin film of SrTiO3 and both impurity doped thin film of SrxLa1-xTiO3 (x=0.1~0.9). Now, we try to deposit of TiO2 on polymer films by laser induced forward transfer method.

4. Synthesis of ZnO nano-films for light emitting device by infrared light excited pulsed laser deposition method

We have synthesis nitrogen doped p-type ZnO nano-films by infrared light excited pulsed laser deposition method. High quality crystalline of p-type ZnO nano-films were improved by pulsed YAG laser annealing below 532 nm of laser wavelength.

5. Bio-electronics

We have studied the sterilization of periodontal bacterium by atmosphere pressure low frequency jet plasma; fresh plasma, and splintering/regeneration of enchytraeus japonensis by irradiation of free electron laser.

6. Green technology

We have studied the evolution of controlled nano/micro bubble by laser/focused ion beam fabricated nozzle on piezoelectric vibrator for defecation of water.

The Development of Newly Molecular Targeting Drug for Prostate Cancer by using PI Polyamide

Daisuke OBINATA, Satoru TAKAHASHI
Medical Group (Department of Urology, School of Medicine)

Under the close collaboration with Noboru Fukuda, Masayoshi Soma, and Kyoko Fujiwara, we have been developing new molecular targeting drug by PI polyamide for cancer therapy.

A recurrent fusion of TMPRSS2 with E26 transformation-specific (ETS) family genes were found in about 80% of prostate cancer tissues. ETS genes are transcription regulators, and altered expression or properties of them affect the control of transcriptional processes. Those alterations also could cause development and progression of cancer. Since TMPRSS2, 5'-fusion partner, was upregulated by androgen, AR has been supposed to be important to regulate the fusion genes in the prostate cancer. Aberrant overexpression of ERG induced by TMPRSS2-ERG fusion is likely to be involved in prostate cancer development. Moreover, recent studies have shown that ligand-dependent binding of AR to intronic binding sites near the specific tumor translocation breakpoints (TGT/AGGGA/T) caused facilitating DNA double-stranded break (DSB) generation.

Pyrrole–imidazole (PI) polyamides are small synthetic molecules that recognize and attach to the minor groove of DNA, followed by inhibition DNA–protein interaction with high affinity and sequence specificity. Synthetic PI polyamides recognize and attach to the minor groove of DNA with high affinity and specificity.

Here, we examined the effects of a PI polyamide targeting TMPRSS2-ERG translocation breakpoints (Fusion Polyamide) on prostate cancer. First, to determinate the binding affinity and specificity of polyamide to target DNA, gel mobility shift assays were performed. The fusion polyamide showed selective DNA binding ability. Human prostate cancer cell line treated with Fusion Polyamide was compared with those with Negative control polyamide. Treatment of Fusion Polyamides showed significant decreased both DHT induced TMPRSS2-ERG and endogeneous ERG expression, as well as cell growth and migration. These results demonstrate that PI polyamide targeting these breakpoints sequences may be a new therapeutic intervention in prostate cancer.

We are now trying to the animal experiment using a nude mouse for elucidating anti-tumor efficacy in vivo.

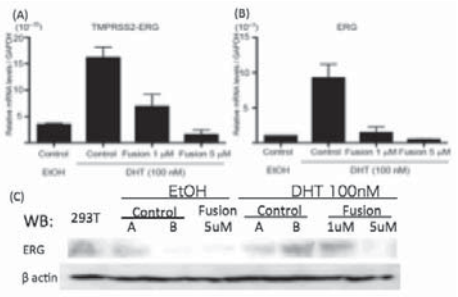

Fig 1. Although TMPRSS2-ERG expression was induced by 100 nM of DHT, treatment of Fusion Polyamides showed significant decreased both TMPRSS2-ERG and endogeneous ERG expression. WB: Western blot

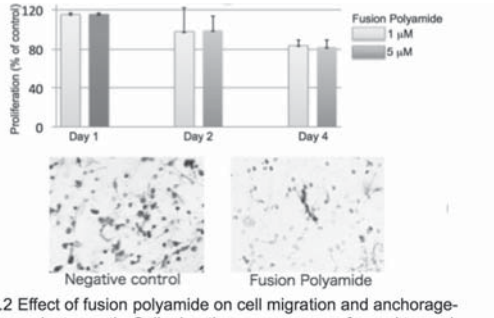

Fig.2 Effect of fusion polyamide on cell migration and anchorage-independent growth. Cell migration assay was performed to analyze the motility of fusion polyamide treated LNCaP cells and control cells. Migrated cells were stained with Giemsa staining solution

Mechanism of Superconductivity in Layered Fe-based Superconductors and Search of New Superconducting Compounds

Yoshiki TAKANO
Nanomaterials and Nanodevices Group

Since $LaFeAsO_{1-x}F_x$ was discovered to be a superconductor in 2008, many iron-based superconductors have been found. Among them, SrFeAsF is called 1111-superconductor and its crystal structure is as same as that of LaFeAsO. When a part of Sr site is substituted by rare earth ions, the superconductivity occurs. In 2010, $RFeAsO_{1-y}$ (R=La, Nd) are also reported to be a superconductor. Then, we have prepared $Sr_{1-x}R_xFeAsF_{1-y}$ (R = La, Nd, Sm) and investigated their superconducting properties. Furthermore, we have investigated the possibility of $Sr_{1-x}Nd_xFeAsF$ for the superconducting wire rod. On the other hand, LiFeAs is called 111-superconductor and is a superconductor with T_c of 18 K itself, which is different from other superconductors. Then, we have tried to prepare $LiFe_{1-x}Co_xAs$ and $Li_{1-x}Y_xFeAs$ and investigated their electrical properties.

1. Superconducting Properties of $Sr_{1-x}R_xFeAsF_{1-y}$ (R=La, Nd, Sm)

The temperature dependence of the electrical resistivity in the normal region is analyzed by a power law such as $r(T)=r_0+AT^n$, where r_0 is the resistivity just above T_c. Figure 1 shows the relation between n and y of $Sr_{1-x}R_xFeAsF_{1-y}$; x = 0.4 for R = La and x = 0.5 for R = Nd and Sm. As F deficiency y increases, n increases. This result is different from the previous study. Figure 2 shows the relation between n and T_c of $Sr_{1-x}R_xFeAsF_{1-y}$. As n increases, T_c decreases. Similar tendency is observed in other iron-based superconductors. It is independent of R ions. While the superconductivity is observed up to y = 0.15 for $Sr_{1-x}La_xFeAsF_{1-y}$ (low T_c compound), the superconductivity disappears at y = 0.05 for $Sr_{1-x}R_xFeAsF_{1-y}$ (R = Nd, Sm) (high T_c compound). n increases rapidly for $Sr_{1-x}R_xFeAsF_{1-y}$ (R = Nd, Sm) in a small y region and it is gradually increases with y for $Sr_{1-x}La_xFeAsF_{1-y}$.

The upper critical magnetic field of $Sr_{0.5}Nd_{0.5}FeAsF$ is higher than that of MgB_2 that has the highest critical current density.

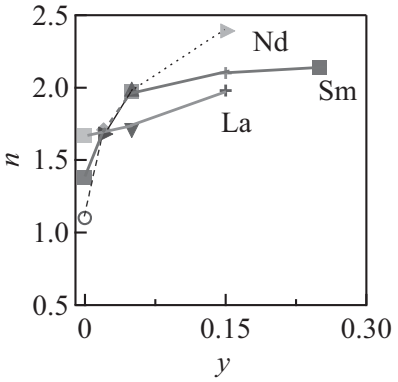

Fig.1 The relation n vs. y.

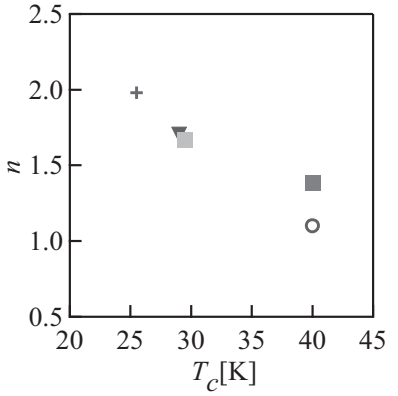

Fig. 2 The relation n vs. T_c .

2. Preparation and Superconductivity of $LiFe_{1-x}Co_xAs$ and $Li_{1-x}Y_xFeAs$

The 111 phases are obtained as main phase. Lattice constants a and c were 3.770Å and 6.358Å for LiFeAs, 3.773Å and 6.350 Å for $LiFe_{0.98}Co_{0.02}As$, and 3.772Å and 6.333 Å for $Li_{0.9}Y_{0.1}FeAs$, respectively. As FeAs is observed as impurities phase, Li is considered to slightly evaporate during sample preparation. T_c of LiFeAs is 10.8K which is smaller than the reported value. T_c of $LiFe_{0.98}Co_{0.02}As$ is 9.5 K and T_c decreased with increasing Co concentration. $Li_{0.9}Y_{0.1}FeAs$ does not show superconductivity above 3 K and the electrical resistivity of normal state also increased.

Ultra Fast Information Recording and Ultra Fast Photo Magnetic Switching

Arata TSUKAMOTO, Akiyoshi ITOH
Information Storage; Supramolecules and Self-Assembly

The ever increasing the capacity of storing information motivates the search for faster approaches to process and magnetically record information. Most computers store data on magnetic hard disk drives, in which the direction – "up" or "down" – of the magnetic moments in a small region of the disk corresponds to a binary bit. However, it was faced to unavoidable fundamental problem for faster operation in conventional way known as ferromagnetic resonance limit. We have experimentally demonstrated that an excitation of magnetization reversal phenomena can be triggered by the ultra-short pulsed laser irradiation. This finding reveals an ultrafast and efficient pathway for writing magnetic bits. Based on deep understanding of relationship between light and magnet including above new discovery, we are striving to establish the fundamental techniques of researching and developing ultrafast spin manipulation.

It has been unexpectedly found that the ultrafast laser-induced spin reversal in GdFeCo, where spins are coupled antiferromagnetically, occurs by way of a transient ferromagnetic-like state (*Nature* 2011). Such a novel strongly non-equilibrium spin dynamics may lead to yet unexplored magnetization reversal. We found that magnetization reversal could be achieved without any magnetic field, using an ultrafast thermal energy load alone (*Nature communications* 2012). Until now it has been generally assumed that heating alone, not represented as a vector at all, cannot result in a deterministic reversal of magnetization, although it may assist this process. We found experimentally deterministic magnetization reversal in a ferrimagnetic GdFeCo driven by an ultrafast heating of the medium resulting from the absorption of a sub-picosecond laser pulse without the presence of a magnetic field. Fig. 1 shows magneto-optical image of magnetic domains after single pulse laser irradiations. Subtracted (difference of each sets of images) images shows various magnetic domain was reversed in same areal size by laser irradiation for all the cases. To exclude the possibility of artifacts caused by dipolar interactions from surrounded magnetic material, arrays of 2 μm diameter disks were fabricated as Fig. 2. The size was chosen so that the structures are much smaller than the laser spot size. The magnetization reversal phenomenon was successfully confirmed. A further set of experiments shows that this switching occurs independently of polarization and initial state in thin films of GdFeCo. Importantly for technological applications, we show experimentally that this type of switching can occur when starting at room temperature.

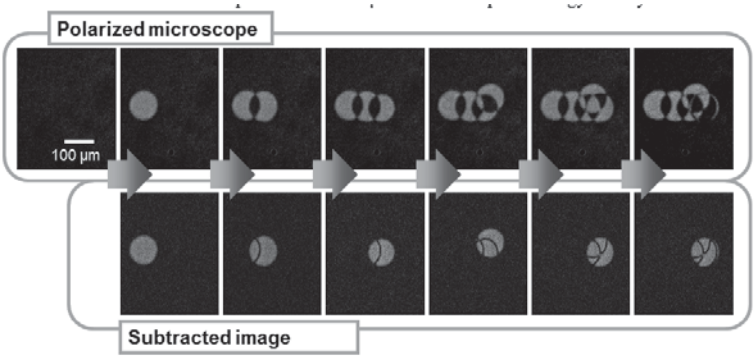

Fig. 1 (a) Magneto-optical image of magnetic domains after single pulse laser irradiations. (b)Subtracted (difference of each sets of images) images.

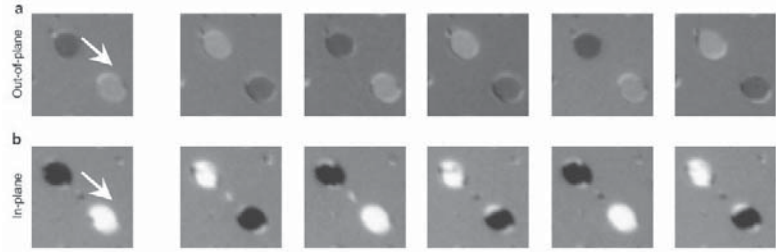

Fig. 2 XMCD images of arrays of 2 μm diameter GdFeCo disks after single pulse laser irradiations (*Nature communications* 2012)

Distribution of Energy Flow by Dielectric Waveguide with Rhombic Dielectric Structures along a Middle Layer –Case of Compared with Deformed Rhombic Dielectric Structure–

Tsuneki YAMASAKI
Quantum Theory and Computation Group

We have analyzed the guiding problem by dielectric waveguides with defects composed of dielectric circular cylinders array and deformed rhombic dielectric structure in the middle layer and investigated the influence of energy flow for defect area by using the propagation constants at the guided region. From the numerical results, it is shown that we can be obtained the confinement efficiency by rhombic dielectric structure compared with deformed rhombic dielectric structures in the middle layer for both TE_0 and TM_0 modes.
These results have been「Reference」as follows:

Reference：
1) R. Ozaki and T. Yamasaki: "Distribution of Energy Flow by Dielectric Waveguide with Rhombic Dielectric Structure along a Middle Layer -Case of Compared with Deformed Rhombic Dielectric Structure-", *IEICE Trans. Electron.*, vol.E96-C, no.1, 2013, (to be published).

●2012 年の業績

○論文：
1) R. Ozaki and T. Yamasaki : Propagation Characteristics of Dielectric Waveguides with Arbitrary Inhomogeneous Media along the Middle Layer, *IEICE Trans. Electron.*, vol.E95-C, no.1, pp.53-62, 2012.
2) R. Ozaki and T. Yamasaki: Distribution of Energy Flow by Dielectric Waveguide with Rhombic Dielectric Structure along a Middle Layer, *IEICE ELEX.,* vol.9, no.7, pp.698-705, 2012.

○国際会議：
1) R. Ozaki and T. Yamasaki : Propagation Characteristics of Dielectric Waveguides with Arbitrary Inhomogeneous Media along the Middle Layer (Part II), *Proc. Progress in Electromagnetic Research Symposium* in Kuala Lumpur, March 27-30, 2012.
2) R. Ozaki and T. Yamasaki : Propagation Characteristics of Dielectric Waveguides with Arbitrary Inhomogeneous Media along the Middle Layer (Part III) , *Proc. Progress in Electromagnetic Research Symposium* in Moscow, August 19-23, 2012.
3) R. Ozaki and T. Yamasaki : Propagation Characteristics and Distribution of Energy Flow by Dielectric Waveguide with Arbitrary Inhomogeneous Media in the Middle Layer, *Proc. 14th International Conference on Mathematical Method in Electromagnetic Theory* in Kharkiv Ukraine, Pl1-2, pp.9-17, August 28-30, 2012.
4) R. Ozaki and T. Yamasaki：Distribution of Energy Flow by Dielectric Waveguide with Rhombic Dielectric Structure along a Middle Layer, *Proc. International Symposium on Antennas and Propagation* in Nagoya, 3D3-2, pp.955-958, Oct.29- Nov.2, 2012.

○研究会・全国大会：
1) 尾崎，山﨑：中空層にひし形誘電体構造をもつ誘電体導波路の伝搬特性とエネルギー分布，電気学会電磁界理論研究会資料，EMT-12-15，pp.57-62，1 月，2012.
2) 尾崎，山﨑：変形ひし形誘電体を中間層に内蔵した誘電体導波路による伝搬特性，電子情報通信学会総合大会講演論文集，C-1-40，3 月，2012.
3) 尾崎，山﨑：エアホール型誘電体導波路による欠陥部のエネルギー分布，電気学会電磁界理論研究会資料，EMT-12-70，pp.29-34 ，5 月，2012.
4) 山﨑，尾崎：フォトニック結晶導波路による電磁波の散乱および導波特性，電子情報通信学会ソサイエティ大会講演論文集，CS-1-2，9 月，2012.
5) 尾崎，山﨑：エアホール型誘電体導波路によるエネルギー分布，電子情報通信学会ソサイエティ大会講演論文集，C-1-8，9 月，2012.
6) 尾崎，山﨑：誘電体円柱とエアホール円柱で構成された多層誘電体導波路による伝搬特性とエネルギー分布，電気学会電磁界理論研究会資料，EMT-12-175，pp.1-6，11 月，2012.